Nanoscale

Accepted Manuscript

This article can be cited before page numbers have been issued, to do this please use: B. Zhi, X. Yao, Y. Cui, G. Orr and C. Haynes, *Nanoscale*, 2019, DOI: 10.1039/C9NR05028K.

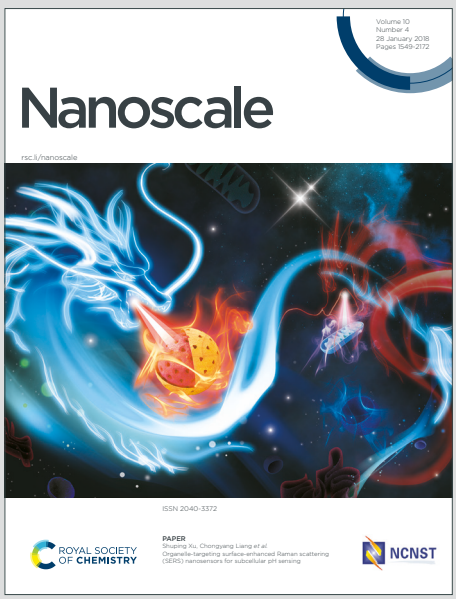

ROYAL SOCIETY OF CHEMISTRY

rsc.li/nanoscale

View Article Online
DOI: 10.1039/C9NR05028K

Synthesis, applications and potential photoluminescence mechanism of spectrally tunable carbon dots

Bo Zhi,[a, %] XiaoXiao Yao,[a, %] Yi Cui,[b,c] Galya Orr,[b] and Christy L. Haynes*[a]

a. Department of Chemistry, University of Minnesota Twin Cities

b. Environmental Molecular Sciences Laboratory, Pacific Northwest National Laboratory, Richland, WA 99354

c. Current address: MIT Media Lab, Cambridge, MA 02139

[%] These authors contributed equally to this work.

*Corresponding author: chaynes@umn.edu

Abstract: Due to the prominent characteristics of carbon-based luminescent nanostructures (known colloquially as carbon dots), such as inexpensive precursors, excellent hydrophilicity, low toxicity, and intrinsic fluorescence, these nanomaterials are regarded as potential candidates to replace traditional quantum dots in some applications. As such, research in the field of carbon dots has been increasing in recent years. In this mini-review, we summarize recent progress in studies of multicolor carbon dots focusing on potential photoluminescence (PL) mechanisms, strategies for effective syntheses, and applications in ion/molecule and temperature sensing, and high-resolution bioimaging techniques.

1. Introduction

The "fluorescent carbon" were accidentally discovered by in 2004 by Xu et al. during electrophoretic analysis and purification of carbon nanotubes.[1] Then Sun et al. successfully synthesized carbon quantum dots in 2006 by passivating carbon nanoparticles with organic molecules such as $PEG1500_N$.[2] Since then, a variety of synthesis methods have been developed, and carbon dots (CDs) are showing great potential as an environmentally friendly substitute for traditional quantum dots in a range of applications. Typically, CD refers to zero-dimensional fluorescent or phosphorescent carbon nanostructures, where the particle size is typically less than 10 nm.[3-6] Up to now, there has not been a well-defined categorization among CDs, but conventionally, CDs with discernible crystalline lattices are named as graphene quantum dots (GQDs with a single graphene layer) or carbon quantum dots (CQDs with multi graphene layers) while CDs with an amorphous nature are named as carbon nanodots (CNDs) or non-conjugated polymeric dots (PDs); specifically, GQDs or CQDs can be synthesized via top-down methods, such as acid treatments of bulk carbon sources (e.g., anthracite coal or carbon black)[7, 8] while a bottom-up approach is usually applied to prepare CNDs or PDs using small organic molecules

View Article Online
DOI: 10.1039/C9NR05028K

such as citric acid and dopamine.[9-11]

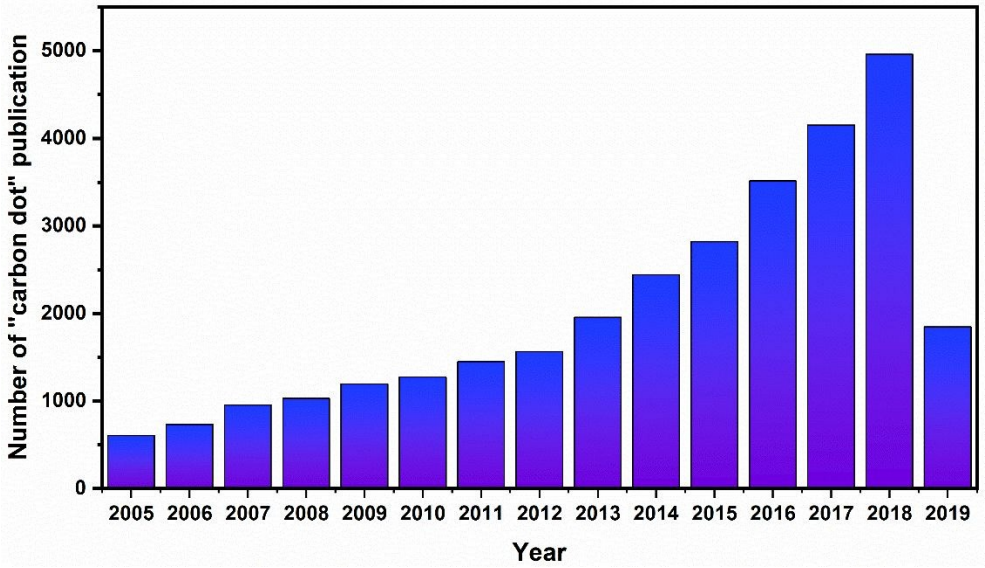

Figure 1. The summary of carbon dot publication since 2005, analyzed via Web of Science up to April 25th, 2019. Search criteria: TOPIC: (carbon dots) OR TOPIC: ("carbon quantum dots") OR TOPIC: ("graphene quantum dots") OR TOPIC: ("carbon nanodots") OR TOPIC: ("non-conjugated polymer dots") NOT TITLE: ("quantum dots").

Typically, CDs are characterized by broad choices of inexpensive precursors, ease of synthesis and surface functionalization, bright luminescence, excellent photostability, and superior biocompatibility.[4, 9, 12, 13] Hence, CDs have the potential to replace traditional semiconductor nanocrystals quantum dots (QDs), which are usually high-cost and raise environmental concerns due to their heavy metal content.[14, 15] Consequently, CDs have become a fast-growing field, attracting an increasing number of researchers to refine synthesis strategies, improve optical and optoelectronic properties, and develop CD-based applications, such as selective sensing,[16-20] target-specific bioimaging,[13, 21-23] environmental remediation,[24] light-emitting diodes (LEDs),[25-29] energy conversion devices,[30-33] and photocatalysis[11, 34, 35]. As shown in the publication analysis (Figure 1), in recent decades, publication efforts on CDs are robust, especially after 2012, making CDs a hot research topic in nanoscience.

At an early stage most of the reported CDs emit intense blue or green luminescence, especially for popular citric-acid based CDs.[5, 36-40] Fortunately, in recent years, publications on multicolour-emitting CDs or long-wavelength-emitting CDs are growing, and quite a few inspiring studies have been reported. Herein, this review will provide a summary of several prevalent hypotheses regarding the origin of the CD PL and synthesis success of multicolor CDs as well as related applications, all topics that are active challenges in the field. The overall goal of this mini-review is to present a clear overview of current achievements and challenges in the field of multicolor CDs.

2. Hypotheses for the PL mechanism of CDs

It is necessary to gain a thorough understanding of the CD luminescence phenomenon before these optical properties can be readily tuned as is possible with traditional QDs. Unfortunately, due to the diversity and complexity of CDs, there is not an accurate description of the CD structure, let alone their photoluminescence mechanism. Up to now, several hypotheses have been proposed to explain the origins of the emission from CDs, such as size-dependent emission

View Article Online
DOI: 10.1039/C9NR05028K

(the quantum confinement effect), surface state-derived luminescence, and embedded molecular luminophores.

2.1. Size-dependent emission

As the particle size distribution of typical CDs (<10 nm) is comparable to the quantum size range, some research groups believe that, similar to the traditional QDs, the size-dependent quantum confinement effect, contributes to the luminescence emission of CDs.[41-46] Yuan and co-workers generated a series of nitrogen-doped, surface-passivated, and highly crystalline CQDs by tuning the fusion and carbonization of citric acid and diaminonaphthalene via a bottom-up solvothermal method.[26] Interestingly, by carefully controlling the synthesis conditions, the emission of the five CQD products were adjusted from blue (430 nm) to red (604 nm). In addition, as the maximum excitation wavelengths were in line with the corresponding excitonic absorption peaks, the authors claimed that the emission should be attributed to band-edge exciton-state decay rather than surface/defect states. Moreover, by carefully examining the particle size and height distribution via TEM and AFM, respectively, it was observed that along with the emission red-shift, the average CD diameters increased from 1.95 nm (blue CDs) to 6.68 nm (red CDs). As such, authors deduced that the red-shifting emission revealed the bandgap transitions in CDs derived from the quantum confinement effect. In our previous work on malic acid-based CDs, we applied reversed-phase column chromatography to separate as-synthesized polymeric CD products (of which the emission was excitation dependent).[21] Three main CD fractions were obtained after the chromatographic purification, emitting blue, turquoise green, and greenish yellow. The size distributions of these CDs were observed to increase from 6.2 ± 2.0 to 9.2 ± 1.7 to 15.6 ± 6.0 nm, corresponding to decreasing optical bandgap energies from 2.97 eV to 2.91 eV to 2.21 eV. Even though the size-dependent emission mechanism is supported in some cases, other studies were unable to find a correlation between size and emission wavelength.[47, 48] Thus, other PL mechanisms are being explored, such as surface state and molecular luminophore.

2.2. Surface state-derived luminescence

Using either top-down or bottom-up synthesis routes, a high temperature (typically 100-200 °C) is necessary to break down carbon precursors or polymerize/carbonize molecular precursors. Therefore, CD reactions are highly reactive (e.g., subject to oxidation and localized carbonization) and consequently, the chemical environments on the CD surfaces are potentially diverse and complicated. One can expect sp^2/sp^3 hybridised carbons, surface defects, and other functional groups.[49-53] As these surface moieties possess different energy levels, some researchers agree that the surface states of CDs should influence the multicolor emissions.[36, 48, 49] Ding and co-workers applied a one-pot hydrothermal method to prepare CD mixtures, and after a thorough chromatographic separation, luminescent CD fractions were obtained covering almost the entire visible range.[54] TEM was used to determine the CD size ranges as well but it was found that the particle size distributions were quite broad. Thus, the authors did not attribute the variable emission properties to the quantum size effect. On the other hand, after carefully comparing the oxygen atom percentages among four representative CD samples, they observed that an increase of carboxyl content and degree of oxidation corresponded with the red shift of CD emissions. As the lowest unoccupied molecular orbital (LUMO) is influenced by oxygen species,[48] they claimed that the band gaps between the highest occupied molecular orbital (HOMO) and LUMO should decrease corresponding to the intensifying surface oxidation of CD samples, leading to a red shift in the PL emission.

View Article Online
DOI: 10.1039/C9NR05028K

2.3. Molecular luminophores

Molecular luminophore-derived emission or molecular state emission is another prevalent hypothesis for CD emission upon preparation by bottom-up methods.[55-60] Considering the existence of active functional groups (e.g., carboxyl and amine groups) within the structures of molecular precursors, these carbon precursors can readily react with one another and undergo further condensation, polymerization, and carbonization, forming the final CD products. However, as bottom-up methods support highly reactive conditions (e.g., a high reaction temperature, high pressure, and/or a long reaction time),[56, 61-63] it is reasonable to expect other side reactions as well. In other words, small molecules or even oligomeric luminophores can be produced during CD synthesis and as such, these luminophores can attach to the surface of CD backbones, granting CDs bright emission characteristics. Recently, Rogach and coworkers hydrothermally synthesized three different CDs by reacting citric acid with three different amine precursors (e.g., ethylenediamine, hexamethylenetetramine, and triethanolamine).[37, 56] They carefully characterized the chemical environments of carbon and nitrogen species within the CDs via X-ray photoelectron spectroscopy, and compared their optical performance with that of citrazinic acid, a molecular fluorophore belonging to the pyridine family. This study confirmed the presence of the derivatives of citrazinic acid and their contribution to the blue fluorescence of ethylenediamine-CDs (e-CDs) and hexamethylenetetramine-CDs (h-CDs). Zhang and co-workers also proposed an intriguing mechanism that the hydrogen bond effect between CD molecular states and solvents may be responsible for the red emission observed from their five CD samples.[64] They prepared five red-emitting CDs by reacting *p*-phenylenediamine in five different polar solvents, namely, water, ethanol, dimethylformamide, cyclohexane, and toluene. Interestingly, due to solvation effects, the CD emission can be adjusted from green to red (540–614 nm). Furthermore, by applying a variety of theoretical models, they thoroughly evaluated the influence of polarization and hydrogen bonding effects on the expected emission variations for the CDs. With these data, they argued that hydrogen bond-dominated molecular state emission was the main mechanism responsible for the spectral shifts. Ferrante and coworkers utilized fluorescence correlation spectroscopy (FCS) and time-resolved electron paramagnetic resonance (TREPR) to study the emission origin of the CDs. FCS showed that the emission of arginine- and citric acid-based CDs were from a molecular entity when excited at 370-440 nm, while the carbonaceous cores was assigned to be the emission origin under 488 nm excitation. The TREPR spectra suggest the presence of aromatic domains in the cores of CDs are responsible for the excited triplet states with a low quantum yield (QY).[65] Examples like this one demonstrate that small fluorescent molecules are often generated in the CD synthesis process, displaying the expected high quantum yields.[58] Thus, adequate CD purification processes must be performed to eliminate emission contributions from small fluorescent molecules.

3. Syntheses of multicolor CDs

Because there is not a decisive understanding about how the CD structure contributes to their luminescence, it remains a challenge to fine-tune the emission wavelengths of the final CD products via adjusting synthesis conditions. Many CDs are known to display interesting excitation-dependent PL behaviour. Namely, the emission of the CDs shift with the increasing excitation wavelength as the intensity usually decreases; in some cases, the optimal emission occurs at the middle excitation wavelength.[66] Thus, the spectrally tunable PL makes CDs a great candidate for multicolour applications. The key point, however, is to synthesize CDs that have emission wavelengths that cover the whole spectrum with good intensity, ideally with QYs

View Article Online
DOI: 10.1039/C9NR05028K

comparable to their QD counterparts. There are several published examples of true multicolor CDs where changing the film thickness or doping concentration facilitates tuning of the emission light from blue to red.[67, 68] Long-wavelength emission (e.g., red or even near infrared regions) is desired because it can provide deeper penetration depths for biological microscopy applications.[69, 70] In fact, quite a number of synthesis successes for multicolor- and long-wavelength-emitting CDs have been reported; this section summarizes these achievements based on the critical synthesis element: precursor screening, solvent engineering, or refining via separation.

3.1. Precursor screening for multicolor CDs

The choice of carbon precursors plays a critical role in the generation of multicolor CDs. Typically, in top-down approaches, bulk carbon sources with crystalline character are chemically or physically "broken down" to obtain GQDs or CQDs. Common precursors include carbon fibers,[71] single/multi- wall carbon nanotubes,[72, 73] and other carbon-rich chemicals.[74, 75] Yuan and co-workers synthesized single-layer and single-crystalline GQDs by refluxing $C_{96}H_{30}$ with fuming nitric acid, followed by hydrothermal treatment at 200 °C.[69] These GQD products exhibited a uniform particle size distribution and more importantly, their optical properties, such as absorption, PL, and two-photon PL, were highly dependent on the size of GQDs; that is, redshifts in emission were observed as the size increased. It is worth noting that an oxidation treatment using phosphoric acid during CD synthesis is nearly a universal component when obtaining long-wavelength-emitting CDs. For example, Gong and co-workers produced N, P-codoped CDs using a one-step acidic oxidation of pumpkin by H_3PO_4.[76] These CDs emitted at 550 nm (yellow fluorescence), corresponding to an optimized excitation of 425 nm. In recent work by Jiang and co-workers, red-emitting CDs were obtained by carbonizing sugar cane bagasse with concentrated H_2SO_4 and H_3PO_4 at 100 °C. Moreover, these CDs can be coated onto polyvinyl fluoride membranes for the fabrication of a solid-state fluorescent vapor sensor, which could selectively detect and quantify the level of toxic ammonia gas.[77]

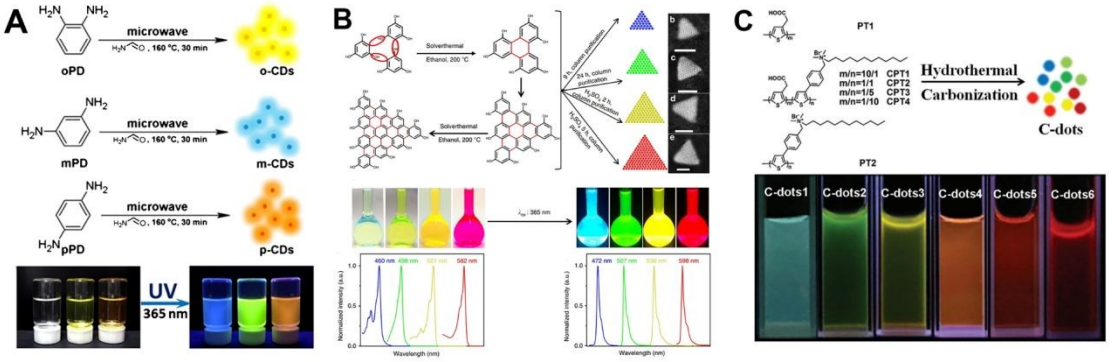

Figure 2. (A) blue, yellow, and orange emitting CDs prepared from phenylenediamine derivatives. This figure has been adapted from ref.78 with permission from Springer. (B) multicolor CQDs obtained by the assembly of phloroglucinol molecules. This figure has been adapted from ref.43 with permission from Springer Nature. (C) the emissions of CDs were tuned from the blue (482 nm) to the near-infrared (680 nm) region by adjusting the ratios of polythiophene derivatives. This figure has been adapted from ref.79 with permission from Royal Society of Chemistry.

Compared to these top-down synthesis, bottom-up methods are typically accomplished using a high-temperature solvothermal environment to assemble molecular or polymer precursors, such as small organic acids, aniline derivatives, phenol derivatives, and polythiophene derivatives, into CD structures.

View Article Online
DOI: 10.1039/C9NR05028K

The most common small organic acid used for the syntheses of CDs is citric acid, originally characterized by emission of intense blue fluorescence;[46, 80-82] however, in recent years, several break-throughs have been reported where citric acid-based CDs can fluoresce in other spectral regions.[27, 83-86] For example, Hola and co-workers reacted citric acid with urea in formamide at 180 °C for 12 hours and then the obtained as-synthesized mixture underwent a chromatographic separation in an anion-exchange column.[83] CD eluents were collected using water and hydrochloric acid as the mobile phase, and the resulting emissions covered the entire visible range. Based on theoretical models, the authors ascribed the multicolor luminescence to the presence of graphitic nitrogen.

In addition to citric acid, aniline derivatives, such as phenylenediamine, are another common molecular precursor that is gaining increasing attention in the last decade.[26, 47, 54, 64, 78, 87-89] Chen and coworkers reported their synthesis work of three different luminescent CDs using o-phenylenediamine, m-phenylenediamine, and *p*-phenylenediamine as carbon sources.[78] The phenylenediamine precursors were dissolved in formamide and heated in a microwave reactor at 160 ˚C for 30 minutes, after which the as-prepared mixtures were further purified by silica column chromatography and dialysis against ethanol. The obtained CD products fluoresced independently of excitation wavelengths, in the blue (444 nm), yellow (533 nm), and orange (574 nm) ranges upon optimized excitations. Based on the facts that the QY was enhanced with increased nitrogen content and that the emission red-shifted with increased C=O/-CONH- content, the authors posit that the luminescence properties are impacted significantly by the surface states, that is, nitrogen-containing functional groups and the degree of oxidation. Liu et.al. chose o-phenylenediamine and phthalic acid as precursors and applied a one-pot solvothermal method to prepare as-synthesized CD mixtures.[88] A subsequent chromatographic purification was conducted to precisely separate them into three different colored products (green, yellow, and orange). After a systematic analysis, the authors suggest that the emission from the green and yellow CDs can be attributed to the quantum size effect while the surface defects induced by oxidation is responsible for the orange-emitting CDs.

In addition to aromatic phenylenediamines, phenol derivatives are also finding increased use in the synthesis of multicolor-emitting CDs.[43, 62, 90-93] Yang and coworkers published their inspiring design of the assembly of phloroglucinol molecules into multicolor triangular CQDs via a six-membered ring cyclization.[43] They skillfully controlled the propagation of the ring cyclization by applying varied amounts of the catalyst, concentrated sulfuric acid, and as such, fine-tuned the sizes of CQDs from 1.9 to 3.9 nm. Along with the increase of the CQD sizes, the emissions red-shifted from 472 to 598 nm and fluoresced four different colors (i.e. blue, green, yellow, and red) corresponding to a decrease in optical bandgap energies from 2.63 to 2.07 eV, which was ascribed to the quantum confinement effect. In addition, as revealed by X-ray powder diffraction, high-angle annular dark field scanning TEM, and high-resolution TEM, the entire set of CQDs exhibited sharp (002) diffraction peaks and well-defined crystalline lattice fringes of the (100) plane, indicative of the highly crystalline nature of these CQD products. Furthermore, DFT simulation studies provided insight that electron-donating hydroxyl groups on the surface of highly crystalline CQD reinforce the charge delocalization and restraine the coupling of electrons and photons, contributing to the high color-purity and narrow emission bandwidth (FWHM of 29-30 nm).

Polymers consisting of aromatic monomers, such as polythiophene derivatives, can also be used to synthesize multicolore CDs.[79, 94-97] Wang and coworkers are taking the lead in designing

View Article Online
DOI: 10.1039/C9NR05028K

tunable multicolor-emitting CDs using polythiophene derivatives as starting agents.[79] In this work, they hydrothermally reacted mixtures of two polythiophene derivatives and, by adjusting the ratios of polythiophene derivatives, the emission of final CD products were tuned from the blue (482 nm) to the near-infrared (680 nm) region while using a single excitation wavelength of 400 nm. Additionally, as these polychromatic CDs exhibited similar size distributions, the authors deduced that the size effect is not responsible for the luminescence. Instead they suggest that differences in CD surface states induced by doping with heteroatoms, such as nitrogen and sulfur, may be responsible and require further investigation.

Overall, though small organic compounds, such as citric acid, used to be the dominating precursors for the preparation of highly luminescent CDs, they tend to yield as-synthesized CD mixtures with extremely complicated compositions, due to their relatively high chemical reactivity and various reaction pathways under high-temperature hydrothermal or solvothermal synthetic conditions. On the other hand, with the goal of achieving some control over the structure of colloidal particles to design multicolor emitting CDs, researchers are more often turning to carbon sources with well-defined molecular structures and relatively predictable reaction routes, such as aromatic compounds that are known to form graphene-like CD structures via controllable syntheses. However, beyond the relatively high expenses of these aromatic chemicals, CD researchers should also be aware of their high toxicity and their potential hazardous influence on the environment and humans.[98-101] Moreover, aniline and phenol derivatives are subject to oxidation in ambient environments[102, 103] and as such, they demand air-free and low-temperature storage conditions, which may eventually increase the synthesis or application cost. Therefore, it remains a challenge and requires further exploration to understand how to prepare these "aromatic" multicolor CDs in an eco-friendly and economical manner as those traditional CDs, such as citric acid-based CDs.

3.2. Solvent engineering for multicolor CDs

Beyond prudent choices of carbon precursors, another effective synthetic strategy to prepare PL-tunable CDs involves solvent engineering; this approach is finding favor with an increasing number of CD researchers.[104-109] Roughly, such a strategy can be divided into two categories: 1) using solvent blends rather than a single solvent as the CD reaction media (“cocktail” solvent engineering)[105, 106] and 2) post-treatment of as-synthesized CDs with varied solvents to take advantage of the solvatochromism of CDs.[107, 108]

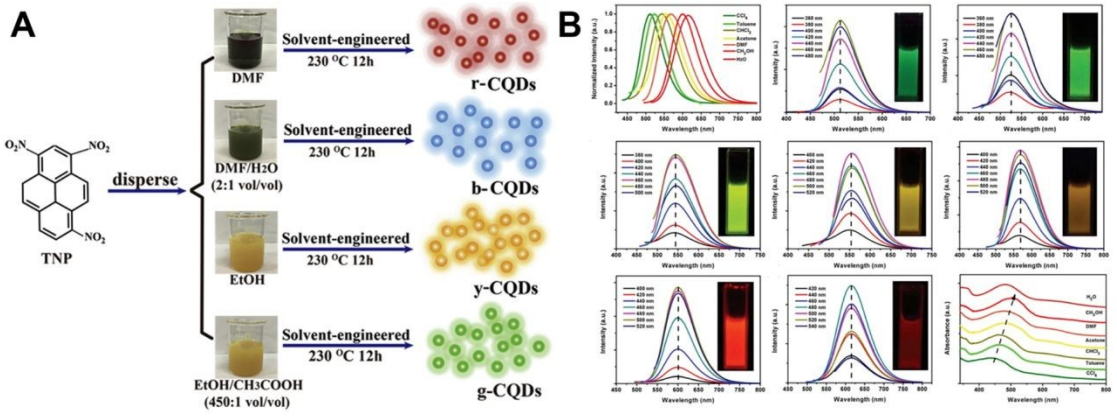

Figure 3. (A) Multicolor CQDs synthesized by tuning the composition and ratios of reaction solvents (water, dimethyl fumarate (DMF), ethanol, and acetic acid). This figure has been adapted from ref.104 with permission from Elsevier.

View Article Online
DOI: 10.1039/C9NR05028K

(B) The solvatochromism of CDs induced by the polarity difference of solvents: CCl_4, toluene, $CHCl_3$, acetone, dimethylformamide, CH_3OH and H_2O. This figure has been adapted from ref.110 with permission from Royal Society of Chemistry.

In the case of the "solvent cocktail" approach, Wu and coworkers recently applied a distinguished molecular fusion strategy and synthesized multicolor CQDs via tuning the composition and ratio of reaction solvents, including water, dimethyl fumarate (DMF), ethanol, and acetic acid.[104] In this way, the bandgaps of CQDs were solvent-engineered from 2.89 down to 2.15 eV, covering the spectral emission range from 460 to 620 nm (Figure 3A). In addition, their optical properties were tested in nonpolar solvents as well to rule out the solvatochromism of CDs induced by the solvent polarity and the spectral characteristics were similar to those of QDs. Solvents were found to alter the elemental composition and functionalization of CDs. Thus they claimed that the mechanism of their multicolor emission should be ascribed to the quantum size effect and surface functional groups. In contrast, though solvatochromism achieved by post-treatment may not be considered a true synthesis approach, it can serve as a convenient and temporary method to tune the emission of CDs in specific solvents.[52, 110-112] The *p*-phenylenediamine-based CDs prepared by Wang and co-workers exhibited solvent-dependent but excitation-independent emissions from 511 to 615 nm (e.g., from dark green to red) upon the dissolution in CCl_4, toluene, $CHCl_3$, acetone, dimethylformamide, CH_3OH and H_2O, respectively (Figure 3B).[110] In addition, based on their X-ray photoelectron spectroscopy and FTIR results, they qualitatively demonstrated that the heteroatoms that are attached to the CD structures, such as nitrogen and oxygen, contribute to an increased charge carrier density, promoting charge transfer of electrons. Therefore, they deduced that these CDs behave like organic dyes, where the arrangement of electrons on the CD surfaces can be affected by the dipole moment of solvents; that is, alongside the increase of solvent polarity, the bandgaps gradually decrease, leading to emission red-shifts.

3.3. Separation or purification methods for as-synthesized CD mixtures

In general, the syntheses for CDs requires a high-temperature (~100 to 250 °C) for either the break-down of bulk carbon (the top-down method) or the carbonization of precursors (the bottom-up method) and so, under such a highly active reaction condition, it is challenging to carefully control of the formation of CDs. As a result, most as-synthesized CD mixtures are composed of unreacted precursors, molecular compounds that are luminescent or not, oligomers or polymers that are carbonized or not, graphene or graphene oxides of varied layers, and amorphous carbons that are doped with heteroatoms or not, depending on the types of carbon sources and reactions.[5, 113-116] Some of these components are photoluminescent while the rest are not and moreover, the fluorescent components can emit distinctive colors upon varied excitation. Thus, even though in recent years, reports about CDs with excitation-independent emission are increasing,[117, 118] as-synthesized CDs are still well-known for their excitation-dependent emission.[49, 52, 119, 120] Under such circumstance, it is necessary to purify or separate CD blends before well-defined CD samples are available for studies of luminescence mechanism or the development of CD-based applications.

Typically, CD researchers perform a two-step post-treatment to refine CD mixtures: 1) a rough purification by dialysis, filtration or centrifugation and 2) a thorough chromatographic separation, such as liquid/liquid extraction (LLE) and solid-phase extraction (SPE).[5, 35, 121]

In most cases, step one is used to remove unreacted starting chemicals, by-products of low molecular weight (MW), and bulk residuals induced by over carbonization. While this first step is usually intended for preparation for the more thorough separation, there are a few reports where

View Article Online
DOI: 10.1039/C9NR05028K

multicolor CDs were obtained in this first step. For example, the as-prepared CDs by Bao and co-workers were synthesized by oxidizing carbon fibers with nitric acid, followed by an effective ultrafiltration of CD.[44] Specifically, multicolor CD fractions (from blue fluorescence to red) were obtained via applying ultrafiltration membranes with an increasing MW equivalents, that is, < 3, 3-10, and 10-30 kDa. And interestingly, the obtained CD particle diameters also showed an increasing tendency: 2.7 ± 0.4, 3.3 ± 0.6, and 4.1 ± 0.6 nm. In addition, the authors carefully examined the influence of reaction time and the concentration of nitric acid, and it turned out that these two factors could lead to emission variation as well. As such, they concluded that both the size effect and the surface oxidation are important for determining the optical properties of their CDs.

For the second step, the separation of CDs via column chromatography often involves liquid/liquid extraction (LLE) or solid-phase extraction (SPE). With the LLE approach, successful separation cases for crude CDs take advantage of normal or reverse phase silica column chromatography, anion-exchange column chromatography, or high-performance liquid chromatography (HPLC).[21, 54, 122, 123] Lin and coworkers recently utilized o-/m- phenylenediamine and tartaric acid as precursors for CD syntheses.[47] The as-synthesized CDs were further purified with a silica column using methylene chloride and methanol as mobile phases, leading to multicolor CD fractions emitting blue, green, yellowish green, and red. Additionally, it was observed that the addition of tartaric acid could induce a red-shifted emission but the size distributions of blue (6.0 nm) and yellowish green (8.2 nm) fractions were larger than those of the green (3.6 nm) and red (4.8 nm) counterparts, as revealed by transmission electron microscopy and atomic force microscopy. As such, the authors inferred that the quantum size effect was not responsible for the luminescent properties, but rather the surface oxidation and carboxylation caused by the addition of tartaric acid. Though LLE methods have become a prevalent strategy for CD post-treatments, the use of a significant amount of organic solvents and the high cost of separation apparatus such as HPLC instruments hamper the scale-up of LLE-based separation techniques. On the other hand, as SPE approaches are less costly and easier to scale-up, they can be another promising option worthy of consideration. Georgakilas and coworkers recently reported their work on the solid-phase separation of as-synthesized CDs using their self-developed aluminium column.[124] To prepare the CDs, citric acid and diamines (e.g., triethylenetetramine and o-phenylenediamine) were chosen as precursors, and their solution in water or ethanol underwent hydrothermal treatment, resulting in the as-prepared mixture. Then, these crude CDs were examined by thin layer chromatography (TLC) to distinguish CDs from undesired organic compounds such as by-products or unreacted precursors. Meanwhile, based on the TLC results, the compositions of mobile phases were optimized for the follow-on SPE operation, leading to a simple and effective purification for violet-, blue-, green-, and yellow-emitting CDs.

As mentioned above, the CD field has largely come to a consensus that it is essential to purify or separate the as-synthesized CDs to achieve refined multicolor CD fractions for further studies. However, due to the complexity of as-synthesized CD mixtures and the lack of understanding the structural details of desired CD fractions, information regarding MW, particle size distributions, particle densities, and particle solubilities are limited. As such, when the first batch of as-synthesized CDs is obtained, researchers face a dilemma: it is difficult to adjust the specifications of their purification apparatus, such as MW cut-off of dialysis membranes, membrane filter pore sizes, centrifugation speed, and suitable mobile phases, until the purification process and subsequent analyses of CD fractions are completed. Accordingly, these purification and analysis

View Article Online
DOI: 10.1039/C9NR05028K

have to be repeated many times until the characteristics of the CD fractions can be completely elucidated, which eventually increases the cost of syntheses and hinders large-scale syntheses. Therefore, it is desirable that the syntheses for multicolor CDs should be free of labour-intensive and time-consuming post treatments.[125, 126] Fortunately, up to now, a few pioneering studies have been published, presenting inspiring work on the separation-free syntheses of multicolor CDs with a high color purity.[43, 127]

4. Applications of multicolor CDs

Akin to other luminescent materials, the emission behaviour of CDs, in essence, refers to the energy transfer between photons and electrons. For practical applications, high QY is desired. For example, high QY makes it possible for the CD emission to compete against the autofluorescence from biological samples. It also helps to achieve higher luminous efficiency in CD-based LEDs. Initially, the QY of CDs was below 10%, but it is increasing and now reached 60 - 81% by optimizing precursors and preparation conditions.[91, 128] As shown in Table 1, the red-emissive CDs are still low QY. Thus further improvements on the QYs are needed to makes CDs competitive for red-emission applications. Here, a summary is provided of the recent progress using multicolor CDs for application in ion/molecule and temperature sensing, modern bioimaging, and CD-based LEDs.

4.1. Selected sensing with CDs

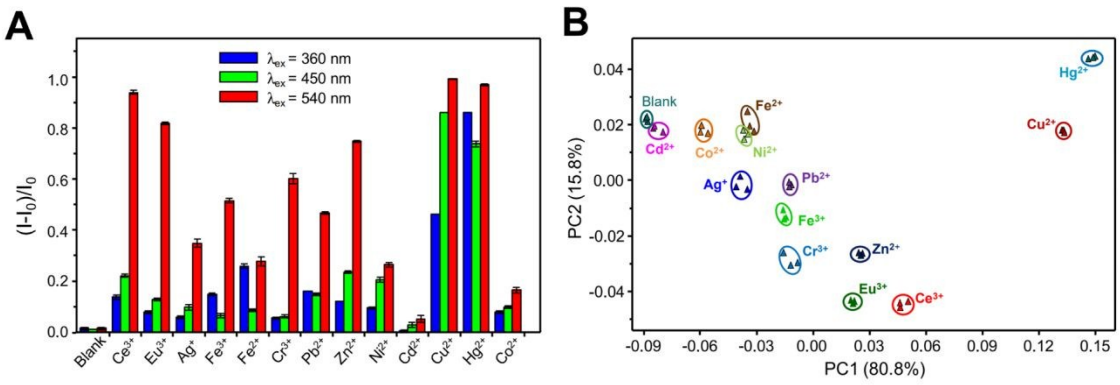

Figure 4. Multicolor CD application in metal ion sensing. (A) Fluorescence emission of CDs at 466, 555, and 637 nm when excited at 360 nm, 450 nm, and 540 nm to 13 metal ions. (B) Principle component analysis of the discrimination of the 13 metal ions based on the fluorescence emission of the CDs. This figure has been adapted from ref. 129 with permission from John Wiley and Sons.

Due to their intrinsic fluorescence, CDs have been developed as sensors for a variety of targets, including pH,[76, 130-132] temperature,[57, 133, 134] metal ions,[129, 133, 135-138] and others.[138-144] In principle, any fluorescence change (e.g. intensity, lifetime, wavelength) which is related to the identity or the concentration of analyte can be developed into sensors.[51] Multicolor CDs with a broad range of emission wavelengths are especially suitable for ratiometric sensing and target discrimination. For example, a CD based ratiometric pH sensor was developed. It shows dual fluorescence emissions where the ratio of emission at 475 nm / 545 nm corresponds linearly to pH from 5.2 to 8.8. This label-free pH nanosensor was used to test intracellular pH in Hela cells.[131] Another ratiometric CD sensor has been developed for multiple targets, temperature, pH and Fe^{3+} ions. Upon 380

View Article Online
DOI: 10.1039/C9NR05028K

nm excitation, the dual fluorescence bands (I_{455nm} / I_{520nm}) was found to decrease with temperature from 10 °C to 82 °C and pH 6.0 to 1.9. It's responsive to Fe^{3+} from 0.04 to 46 μM as well.[145] Ratiometric sensing is self-calibrated and thus avoids many factors that influence measurement of the absolute fluorescence intensity such as the stability of light source and the concentration of CDs.[131]

Carbon dot emission can also be temperature sensitive. CDs synthesized from acrylic acid and methionine have emission between the wavelengths of 440 nm to 555 nm, and the fluorescence intensity correlates linearly to changes in temperature between 25 – 75 °C.[146] In another case, the fluorescence lifetime of N,S co-doped CDs was found to be temperature-dependent and was applied to monitor intracellular temperature.[57] Fluorescence lifetime has advantages over fluorescence intensity in that it is intrinsically referenced. In the same CDs used above, the lifetime of the CDs is not influenced by CD concentration ($1.5x10^{-5}$ to 0.5 mg / mL) or pH (5-12) and is stable for at least 40 h of continuous excitation. An increase in temperature leads to lifetime shortening, and this can be fitted to a 3rd order polynomial calibration curve, where this CD nanothermometer could be used to sense intracellular temperature of HeLa cells.[57]

CDs are also known to be sensitive to various metal ions, including Fe^{3+},[146] Ag^{+},[135] Hg^{+},[137] Cu^{2+},[136] Co^{2+},[147] Pb^{2+},[148] and others.[149-151] Lin and coworkers used CDs synthesized from citric acid and formamide as a multidimensional sensor for metal ions. The emissions of the CDs covered the entire visible range and the QYs are moderately high, 11.9%, 16.7%, and 26.2% under excitation at 360 nm, 450 nm, and 540 nm, respectively. As shown in figure 4, CDs showed different emission intensities in the presence of different metal ions, and these ions can be differentiated properly using principle component analysis.[129] These multicolor CDs could be built into a platform for simultaneous discrimination of multiple metal ions. In another study by Lin and coworkers where multicolor CDs were also made from citric acid and formamide, CDs formed ensembles with the metal ions: Ce^{3+}, Fe^{3+} and Cu^{2+}. These CD-metal ion complexes could effectively distinguish various phosphate anions, such as ATP, ADP AMP, PPi and Pi.[152] This example demonstrates that multicolor CDs could be developed into a platform for sensing and distinguishing different ions as their fluorescence emission at different wavelengths responds differently to presented ions. Other recent representative works are listed in Table 1. Despite these early successes, QY of CDs still need further improvement. Even though the highest QY reported reached 86%,[153] the QY of most CDs are between 2% - 20%.[154] QY is important in developing PL sensors as it reflects the PL intensity that will determine the detection limits and visualization capability.

Table 1: ***CD*** *application in sensing ions and other molecules*

CD emission wavelength	Sensing target	Detection range	Reference

View Article Online
DOI: 10.1039/C9NR05028K

408 nm	glucose	9 - 900 μM	139
450 nm	ascorbic acid	24 - 40 μg/mL	141
455 nm	2, 4, 6-trinitrotoluene	10 nM - 1.5μM	140
510 nm	alkaline phosphate	0.01 to 25 U/L	142
550 nm	H^+	pH 4.7 - 7.4	76
568 nm	Ag^+ and cysteine	1 - 7 μM and 2 - 10 μM	135
594 nm	Fe^{3+}	9.7 nM - 4 μM	155
632 nm	Pt^{2+}, Au^{3+} and Pd^{2+}	0.886, 3.03 and 3.29 μM - 160 μM	156
440 nm and 615 nm	Cu^{2+}	8.82 nM – 225 nM	157

4.2. High-resolution bioimaging with CDs

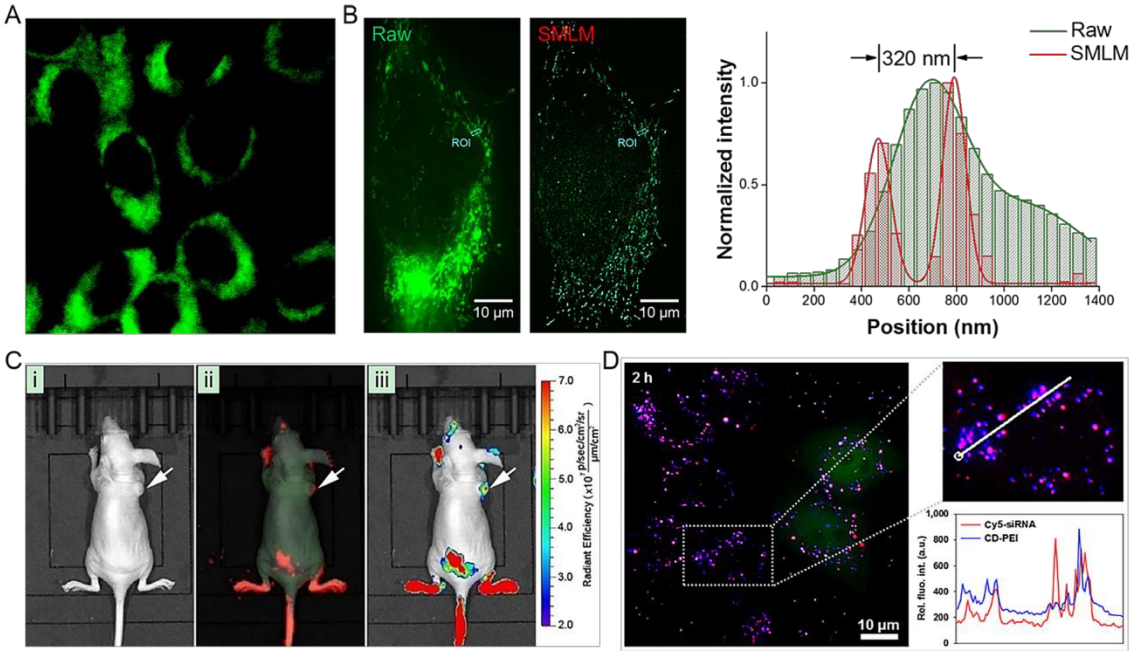

Figure 5. Diverse applications of CDs in bioimaging. (A) Two-photon fluorescence imaging of CDs internalized by human breast cancer cells. This figure has been adapted from ref. 158 with permission from American Chemical Society. (B) Super-resolution single-molecule localization microscopy (SMLM) enabled by photoblinking CDs. The

View Article Online
DOI: 10.1039/C9NR05028K

substantially improved spatial resolution helps resolve closely aligned fine structures within a diffraction-limited area. This figure has been adapted from ref. 21 with permission from American Chemical Society. (C) In vivo tumor imaging with NIR CDs: <i> bright-field image, <ii> fluorescence image, <iii> color-coded image of a nude mouse bearing papillary thyroid carcinoma cells. After 30 min post-intravenous injection, CDs primarily accumulated in bladder and the xenograft tumor site (pointed by arrow). This figure has been adapted from ref. 159 with permission from John Wiley and Sons. (D) CDs used for siRNA delivery. HeLa cells were incubated with passivated CDs (blue) loaded with Cy5-labeled siRNA (red) for 2 h. The co-localization of CDs and Cy5 signals implicate successful delivery. This figure has been adapted from ref. 160 with permission from Springer Nature.

With about two decades' development and optimization, modern CDs feature excellent water solubility, tunable fluorescence emission, sub-10-nm size, superior biocompatibility, and photostability, making them ideal for a broad range of bioimaging applications.[161, 162] Without specific surface modifications, CDs can be readily internalized by different cell types (*e.g.,* plant, bacterial, fungal and cancer cells) (Figure 5A) [163-166] and have been found to localize in various intracellular compartments (*e.g.,* cell membrane, cytoplasm, mitochondria, endosomes and lysosomes),[21, 158, 167, 168] possibly dependent on the different synthesis strategies used to produce the CDs. One prominent advantage of using CDs for bioimaging is their highly efficient uptake by live cells, without apparent toxicity. In addition, the CD surface is often covered with abundant functional groups, such as –COOH and –OH, which can be conveniently modified or conjugated to realize a diversity of sensing/imaging tasks.[169] For example, by covalently binding the CD surface to 4′-(aminomethylphenyl)-2,2′:6′,2″-terpyridine (AE-TPY) molecules, Tian and coworkers produced integrated CD-TPY particles that exhibited pH-dependent fluorescence emission in living cells and tissues of 65-185 μm, where increasing [H^+] potently increases the fluorescence intensity.[170] In another case, *m*-phenylenediamines derived CDs (*m*-CDs) with surface isoquinoline and amines specifically interacted with the major groove of RNA through strong electrostatic force and π–π stacking, which enabled long-term imaging of cellular RNA.[171] To date, surface-modified CDs have also been explored for cancer detection and have shown great promise when cancer-specific markers were targeted, such as the folate receptor.[172-175] Of particular note is the facile production of multicolor CDs from the same precursor, suggesting that similar surface modification chemistry could be exploited to facilitate targeted imaging of more than one target simultaneously.[176-178] All the synthesis and fundamental efforts with CDs facilitate a variety of next-generation biosensing and medical applications.

One inherent challenge constraining conventional optical microscopy is the diffraction-limited spatial resolution (> 200-250 nm). Over the past decade, super-resolution fluorescence microscopy (SRM) has experienced rapid advancement due to the continued development of new instruments and labeling materials.[179] According to their distinct working principles, current super-resolution techniques can be classified into two major groups: patterned illumination-based microscopy (*e.g.,* stimulated emission depletion microscopy (STED) and structured illumination microscopy (SIM)), and single-molecule localization-based microscopy (SMLM) (*i.e.,* stochastic optical reconstruction microscopy (STORM), photo-activated localization microscopy (PALM), or super-resolution optical fluctuation imaging (SOFI)). The first demonstration of SRM using biocompatible CDs was achieved by Pompa and coworkers with the STED technique.[180] In this study, CDs were synthesized by laser ablation and had a peak emission at 490 nm. With the depletion wavelength of 592 nm, a spatial resolution of about 30 nm was achieved both in fixed and live cells. Initially it was thought that the fluorescence emission of CDs was non-intermittent and non-photoblinking.[174] However, a growing body of evidence has revealed that the PL properties of CDs are subject to a large number of factors, and the fluorescence intensity of certain CDs do actively fluctuate in time-lapse experiments.[181-183] The photoblinking of CDs makes them suitable for applications in single-molecule localization-based SRM. Recently, two

View Article Online
DOI: 10.1039/C9NR05028K

studies have characterized the photoblinking properties of as-synthesized CDs.[21, 184] As determined in these studies, as-synthesized CDs exhibited a low on-off duty-cycle (< 1%), high photon output per burst emission (> 6,000), and robust resistance to photobleaching. Taking advantage of these unique properties, SMLM was performed, achieving 25-30 nm spatial resolution (Figure 5B). Moreover, with super-resolution capability, the cellular uptake and transport processes of CDs were better resolved. Representative applications of CDs in SRM are summarized in Table 2.

In addition to the demonstrated potential imaging in cultured cells, CDs have proven to be versatile for *in vivo* imaging as well.[185] By tuning the emission to the near infrared (NIR) range, the biodistribution and toxicology profile of CDs prepared from acid oxidation of carbon nanotubues and graphite has been studied.[186] Moreover, it was found that different injection routes resulted in distinct body distribution and clearance rate.[187] In general, CDs are nontoxic and mainly excreted from the body through the urinary system. Furthermore, CDs have shown strong enhanced permeability and retention (EPR) effect in tumor sites and therefore have been explored as an effective *in vivo* tumor imaging agent (Figure 5C).[159, 174, 188, 189] In light of these findings, CDs can be further functionalized for multimodal *in vivo* applications in conjunction with imaging, considering the abundant reactive groups on their surface. So far, a variety of ideas have been attempted, including targeted chemotherapy, photodynamic therapy, radiation therapy, and gene therapy (Figure 5D).[160, 190-192] Owing to the intrinsic *in vivo* imaging capacity, CD-dependent drug delivery and nanomedicine have the potential to enable real-time tracking, which will greatly facilitate effective drug discovery.

Table 2. Application of CDs in SRM.

Particle size	Imaging method	Cellular localization	Resolution achieved	Ref.
5 nm	STED	lysosome	30 nm (lateral)	180
4 nm	SOFI	nucleus (blue dots); endosomes/lysosomes (green dots)	1.4-fold improvement over wide-field imaging (lateral)	168
4.5 nm	SMLM	microtubule, CCR3 membrane receptor (antibody-based)	25 nm (lateral)	184
5.4 nm	SMLM	nucleolus	4-fold improvement over wide-field imaging (lateral)	193
5 – 15 nm	SMLM	mitochondria	30 nm (lateral)	21

STED: stimulated emission depletion microscopy; SOFI: super-resolution optical fluctuation imaging; SMLM: single-molecule localization microscopy

4.3. CD-based light emitting diodes

The practice of incorporating CDs has attracted substantial attention in optoelectronic devices in addition to their applications in bio-imaging and sensing techniques. Since 2010, CDs have been broadly utilized in light-emitting diodes (LEDs)[194-198], supercapacitors[199-201], lithium ion batteries[202, 203] etc. CDs help to lower the cost and reduce the toxic or rare earth elements that are

View Article Online
DOI: 10.1039/C9NR05028K

conventionally used in optoelectronic devices.[204] So far, tremendous efforts have been made to address the challenges in utilizing CDs as light-emissive components, such as aggregation induced quenching in the solid state and limited wavelength of emission.[204]

Monochromatic LEDs using CDs with a variety of emission colors have been reported.[42, 68, 196, 205] Rogach and coworkers fabricated CD-based ionogel films covering the whole visible spectrum.[67] The same group further constructed LEDs by embedding the CDs in poly(methyl methacrylate) (PMMA), and the emission was tunable from blue to red by altering the film thickness or the doping concentration of CDs (Figure 6A).[68] In another report, aniline-functionalized CDs were embedded in PMMA, acting as a phosphor, that could convert UV excitation to different wavelengths in emission. The emission was successfully tuned to green, yellow, orange and red by using a series of para-substituted aniline-capped CDs. These films had an internal QY of 12-26% and demonstrated excellent photostability after 24 h UV light illumination.[205]

Besides monochromatic LEDs, white LEDs (WLEDs) have also attracted extensive research interest. WLEDs can be prepared either by mixing CDs with different emission wavelengths (e.g., red, green and blue CDs) or utilizing CDs with white emission directly. Yang and coworkers prepared a series of solid CD/starch composites by adjusting their ratios, and the solid composites showed blue, green and yellow emissions, while the solid CDs alone exhibited red emission (Figure 6B). The dichromatic WLEDs were constructed by using the blue CD/starch composite and pure red emissive solid CDs as phosphors.[206] Trichromatic WLEDs were also reported when Xie and coworkers utilized a blue-emissive LED chip (460 nm) and silane-capped CDs with green and red emission as phosphors. The Commission International d'Eclairage (CIE) color coordinates of the trichromatic WLEDs achieved (0.33, 0.30) with a high color rendering index (CRI) of 88.[207] Sun and coworkers utilized blue, green and red CDs excited by an LED chip at 365 nm. They approached CIE of (0.33, 0.34) and CRI of 92.[208] In addition, there are multiple reports on synthesizing white-emissive CDs,[195, 209-212] and surface passivation was found to be important in achieving these white-emissive CDs.[213] Refluxing PAA in glycerol can produce white-emissive CDs with 9% QY. The CDs were coated on a UV chip, and the emission showed CIE of (0.26, 0.30) and CRI of 78.2 (Figure 6C).[211] The above CDs all need UV chip excitation which involves safety concerns as the UV leakage is inevitable.[204] As an alternative, CDs with an electroluminescence (EL) property were developed to act as an active layer in a LED structure. The WLEDs with EL was first fabricated by Wang et al. by synthesizing white-emissive CDs from citric acid, 1-hexdecylamine, and octadecene. The EL spectra cover the whole visible range and is stable to voltage change. The maximum external quantum efficiency achieved 0.083%, which is comparable to commercial semiconductor QD-based WLEDs (Figure 6D).[214] Later, the same CDs were utilized in a different LED structure with a higher maximum brightness of 90 cd/m^2. The EL was reported to be tunable from blue, cyan, magenta to white by varying voltage and device structure.[197]

Though the application of multicolor CDs in LEDs has seen impressive progress, some photophysical properties require further improvement for large-scale use to overcome concerns about photostability, color stability, color rendering capability, and luminous efficiency of LEDs.[204] It has proven difficult to surpass a QY of 30% with multicolor CDs, especially red- and white-emissive CDs which, in turn, limits the luminous performance of LEDs. Taken together, the multicolor CDs have shown great potential in LED fabrication but more efforts are needed to achieve a cost-effective, high-performance product.

View Article Online
DOI: 10.1039/C9NR05028K

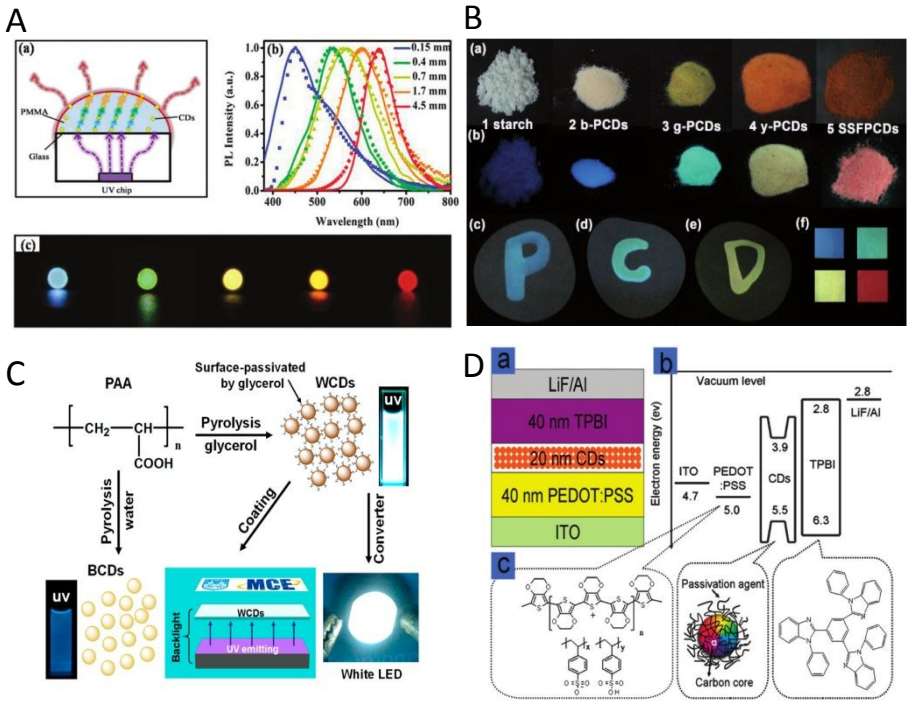

Figure 6. (A) Schematic presentation of CD-based LEDs with different thickness of CD/PMMA films (a), PL spectra of LEDs with CD/PMMA layer thickness increased from 0.15 to 4.5 mm (b), and photo of monochromatic CDs based LEDs of different colors (c). This figure has been adapted from ref 68 with permission from Royal Society of Chemistry. (B) Nanocomposites of CDs and starch under white light (a) and 365 nm UV light (b), photos of fluorescent CDs ink (c-e) and CD/PVA film (f) under 365 nm UV light. This figure has been adapted from ref. 206, licensed under CC BY 4.0. (C) Illustration of the process of white CDs synthesis and its application in WLED. This figure has been adapted from ref. 211 with permission from American Chemical Society. (D) Schematic drawing of the cross-section of CDs-based WLEDs (a), Energy band diagram proposed for the WLEDs (b), and molecular structure of PEDOT:PSS and TPBI (c). This figure has been adapted from ref. 214 with permission from Royal Society of Chemistry.

5. Summary and future directions

In this review, we have summarized what is known about the photoluminescence mechanism, synthesis methods, and separation processes related to spectrally tunable CDs. The applications of multicolour CDs are also presented in terms of sensing, bioimaging, and lighting. Table 3 serves as an easy reference to readers to see the achievements that have been made.

It has been thirteen years since the break-through discovery of carbon-based fluorescent nanostructures in 2006.[2] Due to their fascinating luminescent features, CDs have been attracting an increasing number of researchers to explore the PL mechanisms of their bright emission, preparation of distinct multicolor products independent of excitation, and use in creative applications exploiting their prominent luminescent properties. Many challenges remain, including the lack of thorough interpretation of CD structures and luminescence origins, the difficulty in controlling CD reactions, time-consuming post-treatment procedures, broad emission peaks, and relatively low QYs in the long wavelength emission that limit further applications.[169] However, it is possible that in the near future, studies on mechanisms, optimization of syntheses, and development of applications will benefit from one another and bring about inspiring progress.

One critical next direction for CD researchers is to approach the luminescence mechanism mystery based on experimental analysis of CD structure to figure out how doping, size, or

View Article Online
DOI: 10.1039/C9NR05028K

crystallinity affect the optical properties of CDs.[204] It's desired to use a variety of characterization techniques, including spectroscopy, to further explore the structure-property correlation. In addition, accurate computational simulations that construct theoretical CD models would be an interesting way to predict CD structures. It is also important to further refine the synthesis conditions that are able to produce large scale, highly pure multicolor CDs. Currently, most CD synthetic methods are done on the small scale ,[215] though may have the potential for scale up. In addition, broad emission (large FWHM) are also limiting CD applications, although recent progress has been made to control the FWHM to be around 30 nm.[43] It's also important to design and fabricate CD-based applications to address urgent issues, such as medical or biological devices, environmental monitoring platforms, lighting/display devices, and conversion/storage appliances for sustainable energy. High quantum yields CDs with long-wavelength emissions are needed in bioimaging to produce high quality results. WLEDs have been reported but the field is also pursuing higher color rendering index and better luminescence efficiency. Overall, while we have seen tremendous progress in synthesizing multicolour CDs, CD-related characterization/applications still have a variety of challenges to overcome.

Table 3. A summary of the achievements in multicolor CDs synthesis

Emission Color	Emission Wavelength (nm) or (CIE coordinates)	Quantum Yield	Synthesis Method	Starting Materials	reference
green	515	9.40%	thermal pyrolysis	gram shells	166
green	530	5.8%, 20.1% and 24.4%	hydrothermal treatment	phenol derivatives and ethylenediamine	93
yellow	535	3-6%	acid reflux	single and multi-walled carbon nanotubes, graphite	186
yellow	550	9.42%	acid oxidation	pumpkin	76
yellow	560	0.18%	acid oxidation	sucrose	74
yellow	568	10.8%	solvothermal method	1,2,4-triaminobenzene and formamide	135
orange	590	11.50%	hydrothermal treatment	p-phenylenediamine	117
orange	607	65.93%	solvothermal method	1,3-trinitropyrene	109
red	628	53%	solvothermal method	1,3-dihydroxynaphthalene, KIO4 and ethanol	90
red	630	3%	acid oxidation	sugar cane bagasse	77
red	640	16.2%	solvothermal method	citric acid and formamide	86
red	680	5.40%	hydrothermal treatment	polythiophene derivatives	95
white	(0.31, 0.32)	10%	thermal oxidation	citric acid and LiNO3 salt	209
white	(0.24, 0.31)	9%	thermal pyrolysis	poly(acrylic acid) and glycerol	211

View Article Online
DOI: 10.1039/C9NR05028K

white	(0.40, 0.43)	61%	thermal pyrolysis	citric acid, 1-hexadecylamine and octadecene	214
blue and green	420 and 515	46% and 41%	high temperature treatment	citric acid and urea	168
blue and green	460, 470, and 550	30%, 24%, and 27.6%	microwave heating	malic acid and ethylenediamine	21
blue and green	475 and 545	4.70%	hydrothermal treatment	citric acid and basic fuchsin	131
blue and green	450, 500, 525	2%, 7% and 6%,	acid oxidation	graphite nanofiber	113
blue and orange	420 and 580	10-15% and 20-30%	solvothermal method	p-phenylenediamine and formamide	36
blue and green	455 and 507	21.08% and 54.40%	hydrothermal and solvothermal methods	phthalocyanine	118
green and red	~510 and 604	16.4% and 5.5%	solvothermal method	citric acid or p-phenylenediamine, ethanol and N-(β-aminoethyl)-γ-aminopropyl trimethoxysilane	207
yellow, orange and red	568, 602 and 624	0.7%, 2.5% and 1.4%	acid reflux and hydrothermal treatment	C96H30	69
blue, green and red	425, 540 and 630	52.6%, 35.1% and 12.9%	solvothermal method	citric acid, urea and dimethylformamide	127
blue, green and red	466, 555 and 637	11.9%, 16.7% and 26.2%	solvothermal method	citric acid and formamide	129
blue, green and red	460, 540 and 620	11%-47%	thermal pyrolysis	citric acid, polymethylmethacrylate and N-(β-aminoethyl)-γ-aminopropylmethyldimethoxysilane	68
blue, green and red	435, 535, and 604	4.8%, 10.4% and 20.6%	solvothermal method	phenylenediamine	42
blue, green and red	442, 545 and 620	34%, 19% and 47%	solvothermal method	citric acid and urea	106
blue, green and red	440, 520 and 600	-	acid oxidation	carbon fibers	115
blue to red	450 - 630	4% - 10%	laser ablation and acid reflux to synthesize carbon core followed by	graphite powder, cement and PEG	2

View Article Online
DOI: 10.1039/C9NR05028K

			surface passivation		
blue to red	470 to 670	12.6% (multicolor)	reflux	chloroform and diethylamine	130
blue, green, yellow, orange and red	430, 513, 535, 565, 604	75%, 73%, 58%, 53% and 12%	solvothermal method	citric acid and diaminonaphthalene	26
blue, green, yellow and red	472, 507, 538, 598	66%, 72%, 62% and 54%	solvothermal method	phloroglucinol	43
blue, green, yellow and red	420, 500, 550, 610	-	electrochemical exfoliation and oxidation	graphite	45
blue, green, yellow, red to NIR	435, 510, 535 and 608 with side peaks to 714	4.8%, 28.2%, 10.4% and 22.0%	solvothermal method	phenylenediamine and tartaric acid	47
blue, green, yellow, and orange	425, 500, 548, 558, 575, 580	17%, 17%, 24%, 24%, 26%, 26%	solvothermal method	polyvinylpyrrolidone, urea, citric acid	46
blue, green, red and white	430, 500, 630, (0.30, 0.30)	67% (red), 29% (white)	hydrothermal treatment	citric acid and 5-amino-1,10-phenanthroline	194
violet, blue, green, yellow, orange and red	400, 460, 500, 540, 610 and 710	5%-20%	hydrothermal treatment	citric acid, ethylene glycol and ethylenediamine encapped polyethylenimine	48
UV, blue and green	345, 450, 520,	7.44%, 7.25%, 1.55%	acid reflux and reduction	lamp black	53
blue, green, yellow, red	440, 458, 517, 553, 566, 580, 594, 625	20.51%, 11.75%, 6.18%, 12.69%, 18.83%, 24.50%, 20.33% and 14.19%	hydrothermal treatment	urea, p-phenylenediamine	54
violet, green, yellow	417, 518, 550, 560, 598, 670	4.7%, 3.6%, 3.3%, 2.6%, 4.4%, 3.2%	hydrothermal treatment	p-dihydroxybenzene	62

View Article Online
DOI: 10.1039/C9NR05028K

and red					
violet, blue, green and yellow	417, 457, 497, 537 and 577	49%	thermal pyrolysis	citric acid and [3-(2-aminoethylamino)propyl]trimethoxysilane	67
blue, green and yellow	434, 500 and 564	-	acid exfoliation and etching	carbon fiber	71
blue, yellow and orange	444, 533 and 574	14%, 45% and 8%	solvothermal method	phenylenediamine isomers	78
blue to near IR	482, 524, 570, 609, 628 and 680	-	hydrothermal treatment	polythiophene derivatives	79
blue, green, yellow and red	460, 510, 550 and 630	13.3%, 10.0%, 11.6% and 4.0%	solvothermal method	citric acid, urea and formamide	83
blue, green and yellow	402, 520 and 573	low qy, 16.72%, 38.5%	microwave heating	ortho, meta and para-phenylenediamine	87
green, yellow and orange	529, 547 and 573	39.4%, 11.9% and 9.9%	solvothermal method	phthalic acid, o-phenylenediamine and ethanol	88
blue, green, yellow and red	388, 512, 554 and 625	65.6%, 81.4%, 36.3% and 6.6%	solvothermal method	naphthalenediol, oxidants and ethanol	91
green and yellow-green	515 and 520	27.7% and 28.6%	solvothermal method	m-aminophenol and ethanol	92
blue, green, yellow and red	460, 517, 581 and 620	6.4%, 7.1%, 59.0% and 27.4%	solvothermal method	1,3,6-trinitropyrene	104
blue to NIR	441, 515, 544, 571, 594, 640, 715 and 745	54%(blue), 41%(green), 51%(yellow) and 43%(red)	solvothermal method	L-glutamic acid and o-phenylenediamine	105
violet, blue, green and yellow	433, 435, 500 and 553	23%, 31%, 9.2% and 2.5%	solvothermal method	citric acid, urea and diamines	124
violet, blue and green	390, 495 and 565	-	solvothermal method	3-aminophenylboronic acid	132
violet, blue,	410, 442, 486, 556,	6.2%, 7.2%, 8.4%, 7.6%,	microwave heating	dextrin	177

View Article Online
DOI: 10.1039/C9NR05028K

cyan, green, yellow and deep red	580 and 688	5.1%, 4.8%			
blue, green, yellow, orange and red	430, 513, 535, 565 and 604	75%, 73%, 58%, 53% and 12%	solvothermal method	citric acid, diaminonaphthalene	196
blue, cyan, magenta and white	426, 452, 588 and (0.318, 0.320)	40%	thermal pyrolysis	citric acid, 1-octadecene and 1-hexadecylamine	197
blue, green, yellow and red	460, 510, 575 and 625	18.9%, 8.44%, 5.54% and 8.5%	microwave heating	maleic acid and ethylenediamine	206
blue, orange and white	379, 464 and (0.34, 0.37)	15%, 31% and 7%	calcination	poly(styrene-co-glycidylmethacrylate)	210
blue to red	361, 435, 528, 606 and 714	6.80%	hydrothermal treatment	fructose and HCl	212

Acknowledgements

This work was supported by the National Science Foundation through Chemical Innovation Program, under grant CHE-1503408 for the Center for Sustainable Nanotechnology. Part of this work was done at the Environmental Molecular Sciences Laboratory, a national scientific user facility sponsored by DOE's Office of Biological and Environmental Research and located at Pacific Northwest National Laboratory.

1. X. Xu, R. Ray, Y. Gu, H. J. Ploehn, L. Gearheart, K. Raker and W. A. Scrivens, *J. Am. Chem. Soc.*, 2004, **126**, 12736-12737.
2. Y.-P. Sun, B. Zhou, Y. Lin, W. Wang, K. A. S. Fernando, P. Pathak, M. J. Meziani, B. A. Harruff, X. Wang, H. Wang, P. G. Luo, H. Yang, M. E. Kose, B. Chen, L. M. Veca and S.-Y. Xie, *J. Am. Chem. Soc.*, 2006, **128**, 7756-7757.
3. B. Yao, H. Huang, Y. Liu and Z. Kang, *Trends Chem.*, 2019, **1**, 235-246.
4. L. Xiao and H. Sun, *Nanoscale Horiz.*, 2018, **3**, 565-597.
5. M. Shamsipur, A. Barati and S. Karami, *Carbon*, 2017, **124**, 429-472.
6. J. Li, B. Wang, H. Zhang and J. Yu, *Small*, 2019, **0**, 1805504.
7. Y. Yan, J. Chen, N. Li, J. Tian, K. Li, J. Jiang, J. Liu, Q. Tian and P. Chen, *ACS Nano*, 2018, **12**, 3523-3532.
8. N. Li, A. Than, X. Wang, S. Xu, L. Sun, H. Duan, C. Xu and P. Chen, *ACS Nano*, 2016, **10**, 3622-3629.

View Article Online
DOI: 10.1039/C9NR05028K

9. B. Zhi, M. J. Gallagher, B. P. Frank, T. Y. Lyons, T. A. Qiu, J. Da, A. C. Mensch, R. J. Hamers, Z. Rosenzweig, D. H. Fairbrother and C. L. Haynes, *Carbon*, 2018, **129**, 438-449.
10. J. Li, X. Li, L. Zeng, S. Fan, M. Zhang, W. Sun, X. Chen, M. O. Tadé and S. Liu, *Nanoscale*, 2019, **11**, 3877-3887.
11. Y. Choi, Y. Choi, O.-H. Kwon and B.-S. Kim, *Chem. Asian J.*, 2018, **13**, 586-598.
12. Y. Zhang, A. A. Tamijani, M. E. Taylor, B. Zhi, C. L. Haynes, S. E. Mason and R. J. Hamers, *J. Am. Chem. Soc.*, 2019.
13. M. Pirsaheb, S. Mohammadi, A. Salimi and M. Payandeh, *Microchim. Acta*, 2019, **186**, 231.
14. S. Pramanik, S. K. E. Hill, B. Zhi, N. V. Hudson-Smith, J. J. Wu, J. N. White, E. A. McIntire, V. S. S. K. Kondeti, A. L. Lee, P. J. Bruggeman, U. R. Kortshagen and C. L. Haynes, *Environ. Sci.: Nano*, 2018, **5**, 1890-1901.
15. M. J. Gallagher, J. T. Buchman, T. A. Qiu, B. Zhi, T. Y. Lyons, K. M. Landy, Z. Rosenzweig, C. L. Haynes and D. H. Fairbrother, *Environ. Sci.: Nano*, 2018, **5**, 1694-1710.
16. Z. Zhang, D. Zhang, C. Shi, W. Liu, L. Chen, Y. Miao, J. Diwu, J. Li and S. Wang, *Environ. Sci.: Nano*, 2019.
17. Y. Han, L. Shi, X. Luo, X. Chen, W. Yang, W. Tang, J. Wang, T. Yue and Z. Li, *Carbon*, 2019, **149**, 355-363.
18. R. Su, D. Wang, M. Liu, J. Yan, J.-X. Wang, Q. Zhan, Y. Pu, N. R. Foster and J.-F. Chen, *ACS Omega*, 2018, **3**, 13211-13218.
19. S. D. Pritzl, F. Pschunder, F. Ehrat, S. Bhattacharyya, T. Lohmüller, M. A. Huergo and J. Feldmann, *Nano Lett.*, 2019, **19**, 3886-3891.
20. C. H. Li, R. S. Li, C. M. Li, C. Z. Huang and S. J. Zhen, *Chem. Comm.*, 2019, **55**, 6437-6440.
21. B. Zhi, Y. Cui, S. Wang, B. P. Frank, D. N. Williams, R. P. Brown, E. S. Melby, R. J. Hamers, Z. Rosenzweig, D. H. Fairbrother, G. Orr and C. L. Haynes, *ACS Nano*, 2018, **12**, 5741-5752.
22. H. Liu, Y. Sun, Z. Li, J. Yang, A. A. Aryee, L. Qu, D. Du and Y. Lin, *Nanoscale*, 2019, **11**, 8458-8463.
23. J. Wang, X. Hu, H. Ding, X. Huang, M. Xu, Z. Li, D. Wang, X. Yan, Y. Lu, Y. Xu, Y. Chen, P. C. Morais, Y. Tian, R. Q. Zhang and H. Bi, *ACS Appl. Mater. Interfaces*, 2019, **11**, 18203-18212.
24. L. Xiao, H. Guo, S. Wang, J. Li, Y. Wang and B. Xing, *Environ. Sci.: Nano*, 2019, **6**, 1493-1506.
25. A. Pyne, S. Layek, A. Patra and N. Sarkar, *J. Mater. Chem. C*, 2019, **7**, 6414-6425.
26. Y. Fanglong, W. Zhibin, L. Xiaohong, L. Yunchao, T. Zhan'ao, F. Louzhen and Y. Shihe, *Adv. Mater.*, 2017, **29**, 1604436.
27. T. Hu, Z. Wen, C. Wang, T. Thomas, C. Wang, Q. Song and M. Yang, *Nanoscale Adv.*, 2019, **1**, 1413-1420.
28. E. Liu, D. Li, X. Zhou, G. Zhou, H. Xiao, D. Zhou, P. Tian, R. Guo and S. Qu, *ACS Sustain. Chem. Eng*, 2019, **7**, 9301-9308.
29. X. Feng, K. Jiang, H. Zeng and H. Lin, *Nanomaterials*, 2019, **9**, 725.
30. L. Vallan, R. Canton-Vitoria, H. B. Gobeze, Y. Jang, R. Arenal, A. M. Benito, W. K. Maser, F. D'Souza and N. Tagmatarchis, *J. Am. Chem. Soc.*, 2018, **140**, 13488-13496.
31. D. Kong, Y. Wang, S. Huang, Y. V. Lim, J. Zhang, L. Sun, B. Liu, T. Chen, P. Valdivia y Alvarado and H. Y. Yang, *J. Mater. Chem. A*, 2019, **7**, 12751-12762.
32. J. B. Essner and G. A. Baker, *Environ. Sci.: Nano*, 2017, **4**, 1216-1263.
33. J. T. Margraf, F. Lodermeyer, V. Strauss, P. Haines, J. Walter, W. Peukert, R. D. Costa, T. Clark and D. M. Guldi, *Nanoscale Horiz.*, 2016, **1**, 220-226.

View Article Online
DOI: 10.1039/C9NR05028K

34. G. A. M. Hutton, B. C. M. Martindale and E. Reisner, *Chem. Soc. Rev.*, 2017, **46**, 6111-6123.
35. C. Hu, M. Li, J. Qiu and Y.-P. Sun, *Chem. Soc. Rev.*, 2019, **48**, 2315-2337.
36. D. Chen, H. Gao, X. Chen, G. Fang, S. Yuan and Y. Yuan, *ACS Photonics*, 2017, **4**, 2352-2358.
37. J. Schneider, C. J. Reckmeier, Y. Xiong, M. von Seckendorff, A. S. Susha, P. Kasák and A. L. Rogach, *J. Phys. Chem. C*, 2017, **121**, 2014-2022.
38. Z. L. Wu, Z. X. Liu and Y. H. Yuan, *J. Mater. Chem. B*, 2017, **5**, 3794-3809.
39. Z. Sun, X. Li, Y. Wu, C. Wei and H. Zeng, *New J. Chem.*, 2018, **42**, 4603-4611.
40. L. Vallan, E. P. Urriolabeitia, F. Ruipérez, J. M. Matxain, R. Canton-Vitoria, N. Tagmatarchis, A. M. Benito and W. K. Maser, *J. Am. Chem. Soc.*, 2018, **140**, 12862-12869.
41. O. Kozák, M. Sudolská, G. Pramanik, P. Cígler, M. Otyepka and R. Zbořil, *Chem. Mater.*, 2016, **28**, 4085-4128.
42. K. Jiang, S. Sun, L. Zhang, Y. Lu, A. Wu, C. Cai and H. Lin, *Angew. Chem. Int. Ed.*, 2015, **54**, 5360-5363.
43. F. Yuan, T. Yuan, L. Sui, Z. Wang, Z. Xi, Y. Li, X. Li, L. Fan, Z. a. Tan, A. Chen, M. Jin and S. Yang, *Nat. Commun.*, 2018, **9**, 2249.
44. L. Bao, C. Liu, Z.-L. Zhang and D.-W. Pang, *Adv. Mater.*, 2015, **27**, 1663-1667.
45. X. Tan, Y. Li, X. Li, S. Zhou, L. Fan and S. Yang, *Chem. Commun.*, 2015, **51**, 2544-2546.
46. J. Zhu, X. Bai, X. Chen, H. Shao, Y. Zhai, G. Pan, H. Zhang, E. V. Ushakova, Y. Zhang, H. Song and A. L. Rogach, *Adv. Opt. Mater.*, 2019, **7**, 1801599.
47. K. Jiang, X. Feng, X. Gao, Y. Wang, C. Cai, Z. Li and H. Lin, *Nanomaterials*, 2019, **9**, 529.
48. S. Hu, A. Trinchi, P. Atkin and I. Cole, *Angew. Chem. Int. Ed.*, 2015, **54**, 2970-2974.
49. S. Y. Lim, W. Shen and Z. Q. Gao, *Chem. Soc. Rev.*, 2015, **44**, 362-381.
50. S. Hu, *Chem. Rec.*, 2016, **16**, 219-230.
51. X. Sun and Y. Lei, *Trends Anal. Chem.*, 2017, **89**, 163-180.
52. P. M. Gharat, J. M. Chethodil, A. P. Srivastava, P. P. K, H. Pal and S. Dutta Choudhury, *Photochem. Photobiol. Sci.*, 2019, **18**, 110-119.
53. D. Shen, Y. Long, J. Wang, Y. Yu, J. Pi, L. Yang and H. Zheng, *Nanoscale*, 2019, **11**, 5998-6003.
54. H. Ding, S. B. Yu, J. S. Wei and H. M. Xiong, *ACS Nano*, 2016, **10**, 484-491.
55. Y. Song, S. Zhu, S. Zhang, Y. Fu, L. Wang, X. Zhao and B. Yang, *J. Mater. Chem. C*, 2015, **3**, 5976-5984.
56. Y. Xiong, J. Schneider, E. V. Ushakova and A. L. Rogach, *Nano Today*, 2018, **23**, 124-139.
57. S. Kalytchuk, K. Poláková, Y. Wang, J. P. Froning, K. Cepe, A. L. Rogach and R. Zbořil, *ACS Nano*, 2017, **11**, 1432-1442.
58. J. B. Essner, J. A. Kist, L. Polo-Parada and G. A. Baker, *Chem. Mater.*, 2018, **30**, 1878-1887.
59. K. Mishra, S. Koley and S. Ghosh, *J. Phys. Chem. Lett.*, 2019, **10**, 335-345.
60. M. Shamsipur, A. Barati, A. A. Taherpour and M. Jamshidi, *J. Phys. Chem. Lett.*, 2018, **9**, 4189-4198.
61. J. Du, N. Xu, J. Fan, W. Sun and X. Peng, *Small*, 2019, 1805087.
62. Y. Wang, Q. Su and X. Yang, *Chem. Commun.*, 2018, **54**, 11312-11315.
63. V. Mishra, A. Patil, S. Thakur and P. Kesharwani, *Drug Discov. Today*, 2018, **23**, 1219-1232.
64. T. Zhang, J. Zhu, Y. Zhai, H. Wang, X. Bai, B. Dong, H. Wang and H. Song, *Nanoscale*, 2017, **9**, 13042-13051.

View Article Online
DOI: 10.1039/C9NR05028K

65. M. Righetto, A. Privitera, I. Fortunati, D. Mosconi, M. Zerbetto, M. L. Curri, M. Corricelli, A. Moretto, S. Agnoli, L. Franco, R. Bozio and C. Ferrante, *J. Phys. Chem. Lett.*, 2017, **8**, 2236-2242.
66. Z. Gan, H. Xu and Y. Hao, *Nanoscale*, 2016, **8**, 7794-7807.
67. Y. Wang, S. Kalytchuk, Y. Zhang, H. Shi, S. V. Kershaw and A. L. Rogach, *J. Phys. Chem. Lett.*, 2014, **5**, 1412-1420.
68. C. Sun, Y. Zhang, S. Kalytchuk, Y. Wang, X. Zhang, W. Gao, J. Zhao, K. Cepe, R. Zboril, W. W. Yu and A. L. Rogach, *J. Mater. Chem. C*, 2015, **3**, 6613-6615.
69. B. Yuan, X. Sun, J. Yan, Z. Xie, P. Chen and S. Zhou, *Phys. Chem. Chem. Phys.*, 2016, **18**, 25002-25009.
70. J. V. Frangioni, *Curr. Opin. Chem. Biol.*, 2003, **7**, 626-634.
71. J. Peng, W. Gao, B. K. Gupta, Z. Liu, R. Romero-Aburto, L. Ge, L. Song, L. B. Alemany, X. Zhan, G. Gao, S. A. Vithayathil, B. A. Kaipparettu, A. A. Marti, T. Hayashi, J.-J. Zhu and P. M. Ajayan, *Nano Lett.*, 2012, **12**, 844-849.
72. Y. Dong, H. Pang, S. Ren, C. Chen, Y. Chi and T. Yu, *Carbon*, 2013, **64**, 245-251.
73. W. Chen, F. Li, C. Wu and T. Guo, *Appl. Phys. Lett.*, 2014, **104**, 063109.
74. M. M. F. Chang, I. R. Ginjom, M. Ngu-Schwemlein and S. M. Ng, *Microchim. Acta*, 2016, **183**, 1899-1907.
75. T. Yuan, T. Meng, P. He, Y. Shi, Y. Li, X. Li, L. Fan and S. Yang, *J. Mater. Chem. C*, 2019, **7**, 6820-6835.
76. X. Gong, W. Lu, Y. Liu, Z. Li, S. Shuang, C. Dong and M. M. F. Choi, *J. Mater. Chem. B*, 2015, **3**, 6813-6819.
77. B.-P. Jiang, B. Zhou, X.-C. Shen, Y.-X. Yu, S.-C. Ji, C.-C. Wen and H. Liang, *Chem.: Eur. J.*, 2015, **21**, 18993-18999.
78. C. Liu, R. Wang, B. Wang, Z. Deng, Y. Jin, Y. Kang and J. Chen, *Microchim. Acta*, 2018, **185**, 539.
79. L. Guo, J. Ge, W. Liu, G. Niu, Q. Jia, H. Wang and P. Wang, *Nanoscale*, 2016, **8**, 729-734.
80. N. Dhenadhayalan, K.-C. Lin, R. Suresh and P. Ramamurthy, *J. Phys. Chem. C*, 2016, **120**, 1252-1261.
81. F. Gao, S. Ma, J. Li, K. Dai, X. Xiao, D. Zhao and W. Gong, *Carbon*, 2017, **112**, 131-141.
82. Q. Fang, Y. Dong, Y. Chen, C.-H. Lu, Y. Chi, H.-H. Yang and T. Yu, *Carbon*, 2017, **118**, 319-326.
83. K. Holá, M. Sudolská, S. Kalytchuk, D. Nachtigallová, A. L. Rogach, M. Otyepka and R. Zbořil, *ACS Nano*, 2017, **11**, 12402-12410.
84. B. Wang, Y. Wang, H. Wu, X. Song, X. Guo, D. Zhang, X. Ma and M. Tan, *RSC Adv.*, 2014, **4**, 49960-49963.
85. D. Qu, M. Zheng, P. Du, Y. Zhou, L. Zhang, D. Li, H. Tan, Z. Zhao, Z. Xie and Z. Sun, *Nanoscale*, 2013, **5**, 12272-12277.
86. S. Sun, L. Zhang, K. Jiang, A. Wu and H. Lin, *Chem. Mater.*, 2016, **28**, 8659-8668.
87. L. Song, Y. Cui, C. Zhang, Z. Hu and X. Liu, *RSC Adv.*, 2016, **6**, 17704-17712.
88. Y. Ding, J. Zheng, J. Wang, Y. Yang and X. Liu, *J. Mater. Chem. C*, 2019, **7**, 1502-1509.
89. C. Reckmeier, J. Schneider, A. Susha and A. Rogach, *Opt. Express*, 2016, **24**, A312-A340.
90. Z. Wang, F. Yuan, X. Li, Y. Li, H. Zhong, L. Fan and S. Yang, *Adv. Mater.*, 2017, **29**, 1702910.
91. W. Zhu, X. Meng, H. Li, F. He, L. Wang, H. Xu, Y. Huang, W. Zhang, X. Fang and T. Ding, *Opt. Mater.*, 2019, **88**, 412-416.
92. Q. Wang, S. Zhang, Y. Zhong, X.-F. Yang, Z. Li and H. Li, *Anal. Chem.*, 2017, **89**, 1734-1741.

View Article Online
DOI: 10.1039/C9NR05028K

93. Q. Liu, D. Li, Z. Zhu, S. Yu, Y. Zhang, D. Yu and Y. Jiang, *RSC Adv.*, 2018, **8**, 4850-4856.
94. Z. Liu, A. Nahhas, L. Liu, E. Ada, X. Zhang and S. K. Manohar, *J. Nanomater.*, 2018, **2018**, 7.
95. J. Ge, M. Lan, B. Zhou, W. Liu, L. Guo, H. Wang, Q. Jia, G. Niu, X. Huang, H. Zhou, X. Meng, P. Wang, C.-S. Lee, W. Zhang and X. Han, *Nat. Commun.*, 2014, **5**, 4596-4596.
96. L. Meng, M. Lan, L. Guo, L. Xie, W. Hui, J. Ge, W. Liu, Y. Wang and P. Wang, *RSC Adv.*, 2015, **5**, 26886-26890.
97. J. Ge, Q. Jia, W. Liu, L. Guo, Q. Liu, M. Lan, H. Zhang, X. Meng and P. Wang, *Adv. Mater.*, 2015, **27**, 4169-4177.
98. F. Jenkins, J. Robinson, J. Gellatly and G. Salmond, *Food Cosmet Toxicol.*, 1972, **10**, 671-679.
99. J. Bus and J. Popp, *Food Chem. Toxicol.*, 1987, **25**, 619-626.
100. T. Tišler and J. Zagorc-Končan, *Water Air Soil Pollut.*, 1997, **97**, 315-322.
101. G. Pedersen, J. Brynskov and T. Saermark, *Scand. J. Gastroenterol.*, 2002, **37**, 74-79.
102. Z. D. Zujovic, L. Zhang, G. A. Bowmaker, P. A. Kilmartin and J. Travas-Sejdic, *Macromolecules*, 2008, **41**, 3125-3135.
103. J. Zazo, J. Casas, A. Mohedano, M. Gilarranz and J. Rodriguez, *Environ. Sci. Technol.*, 2005, **39**, 9295-9302.
104. J. Zhan, B. J. Geng, K. Wu, G. Xu, L. Wang, R. Y. Guo, B. Lei, F. F. Zheng, D. Y. Pan and M. H. Wu, *Carbon*, 2018, **130**, 153-163.
105. H. Ding, J.-S. Wei, P. Zhang, Z.-Y. Zhou, Q.-Y. Gao and H.-M. Xiong, *Small*, 2018, **14**, 1800612.
106. J. Zhu, X. Bai, J. Bai, G. Pan, Y. Zhu, Y. Zhai, H. Shao, X. Chen, B. Dong, H. Zhang and H. Song, *Nanotechnology*, 2018, **29**, 085705.
107. M. Zheng, Y. Li, Y. Zhang and Z. Xie, *RSC Adv.*, 2016, **6**, 83501-83504.
108. C. J. Reckmeier, Y. Wang, R. Zboril and A. L. Rogach, *J. Phys. Chem. C*, 2016, **120**, 10591-10604.
109. M. Wu, J. Zhan, B. Geng, P. He, K. Wu, L. Wang, G. Xu, Z. Li, L. Yin and D. Pan, *Nanoscale*, 2017, **9**, 13195-13202.
110. H. Wang, C. Sun, X. Chen, Y. Zhang, V. L. Colvin, Q. Rice, J. Seo, S. Feng, S. Wang and W. W. Yu, *Nanoscale*, 2017, **9**, 1909-1915.
111. A. Sciortino, E. Marino, B. v. Dam, P. Schall, M. Cannas and F. Messina, *J. Phys. Chem. Lett.*, 2016, **7**, 3419-3423.
112. P. Jing, D. Han, D. Li, D. Zhou, D. Shen, G. Xiao, B. Zou and S. Qu, *Nanoscale Horiz.*, 2018, **4**, 175-181.
113. J. C. Vinci, I. M. Ferrer, S. J. Seedhouse, A. K. Bourdon, J. M. Reynard, B. A. Foster, F. V. Bright and L. A. Colón, *J. Phys. Chem. Lett.*, 2012, **4**, 239-243.
114. F. Arcudi, L. Đorđević and M. Prato, *Angew. Chem. Int. Ed.*, 2016, **55**, 2107-2112.
115. N. Fuyuno, D. Kozawa, Y. Miyauchi, S. Mouri, R. Kitaura, H. Shinohara, T. Yasuda, N. Komatsu and K. Matsuda, *Adv. Opt. Mater.*, 2014, **2**, 983-989.
116. Y. Zhou, P. Y. Liyanage, D. L. Geleroff, Z. Peng, K. J. Mintz, S. D. Hettiarachchi, R. R. Pandey, C. C. Chusuei, P. L. Blackwelder and R. M. Leblanc, *ChemPhysChem*, 2018, **19**, 2589-2597.
117. Y. Jiao, X. Gong, H. Han, Y. Gao, W. Lu, Y. Liu, M. Xian, S. Shuang and C. Dong, *Anal. Chim. Acta*, 2018, **1042**, 125-132.
118. P. Lesani, S. M. Ardekani, A. Dehghani, M. Hassan and V. G. Gomes, *Sens. Actuators B Chem.*, 2019, **285**, 145-155.
119. A. A. Kokorina, E. S. Prikhozhdenko, N. V. Tarakina, A. V. Sapelkin, G. B. Sukhorukov and I. Y. Goryacheva, *Carbon*, 2018, **127**, 541-547.

View Article Online
DOI: 10.1039/C9NR05028K

120. P. Zhao, X. Li, G. Baryshnikov, B. Wu, H. Ågren, J. Zhang and L. Zhu, *Chem. Sci.*, 2018, **9**, 1323-1329.
121. K. J. Mintz, Y. Zhou and R. M. Leblanc, *Nanoscale*, 2019, **11**, 4634-4652.
122. L. Liu and Z. Xu, *Anal. Methods*, 2019, **11**, 760-766.
123. C.-Y. Chen, Y.-H. Tsai and C.-W. Chang, *New J. Chem.*, 2019, **43**, 6153-6159.
124. A. Koutsioukis, A. Akouros, R. Zboril and V. Georgakilas, *Nanoscale*, 2018, **10**, 11293-11296.
125. A. Blumer, A. Ehrenfeucht, D. Haussler and M. K. Warmuth, *Inf. Process. Lett.*, 1987, **24**, 377-380.
126. P. Domingos, *Data Min. Knowl. Discov.*, 1999, **3**, 409-425.
127. X. Miao, D. Qu, D. Yang, B. Nie, Y. Zhao, H. Fan and Z. Sun, *Advanced Materials*, 2018, **30**, 1704740.
128. L.-M. Shen and J. Liu, *Talanta*, 2016, **156-157**, 245-256.
129. L. Pan, S. Sun, A. Zhang, K. Jiang, L. Zhang, C. Dong, Q. Huang, A. Wu and H. Lin, *Adv. Mater.*, 2015, **27**, 7782-7787.
130. H. Nie, M. Li, Q. Li, S. Liang, Y. Tan, L. Sheng, W. Shi and S. X.-A. Zhang, *Chem. Mater.*, 2014, **26**, 3104-3112.
131. J. Shangguan, D. He, X. He, K. Wang, F. Xu, J. Liu, J. Tang, X. Yang and J. Huang, *Anal. Chem.*, 2016, **88**, 7837-7843.
132. Y. Wang, L. Lu, H. Peng, J. Xu, F. Wang, R. Qi, Z. Xu and W. Zhang, *Chem. Commun.*, 2016, **52**, 9247-9250.
133. C. Wang, Z. Xu, H. Cheng, H. Lin, M. G. Humphrey and C. Zhang, *Carbon*, 2015, **82**, 87-95.
134. W. Liu, S. Xu, Z. Li, R. Liang, M. Wei, D. G. Evans and X. Duan, *Chem. Mater.*, 2016, **28**, 5426-5431.
135. K. Jiang, S. Sun, L. Zhang, Y. Wang, C. Cai and H. Lin, *ACS Appl. Mater. Interfaces*, 2015, **7**, 23231-23238.
136. J. Chen, Y. Li, K. Lv, W. Zhong, H. Wang, Z. Wu, P. Yi and J. Jiang, *Sens. Actuators B Chem.*, 2016, **224**, 298-306.
137. J. He, H. Zhang, J. Zou, Y. Liu, J. Zhuang, Y. Xiao and B. Lei, *Biosens. Bioelectron.*, 2016, **79**, 531-535.
138. N. Wang, Y. Wang, T. Guo, T. Yang, M. Chen and J. Wang, *Biosens. Bioelectron.*, 2016, **85**, 68-75.
139. P. Shen and Y. Xia, *Anal. Chem.*, 2014, **86**, 5323-5329.
140. L. Zhang, Y. Han, J. Zhu, Y. Zhai and S. Dong, *Anal. Chem.*, 2015, **87**, 2033-2036.
141. J. F. Y. Fong, S. F. Chin and S. M. Ng, *Biosens. Bioelectron.*, 2016, **85**, 844-852.
142. G. Li, H. Fu, X. Chen, P. Gong, G. Chen, L. Xia, H. Wang, J. You and Y. Wu, *Anal. Chem.*, 2016, **88**, 2720-2726.
143. H. Li, C. Sun, R. Vijayaraghavan, F. Zhou, X. Zhang and D. R. MacFarlane, *Carbon*, 2016, **104**, 33-39.
144. X. Yan, Y. Song, C. Zhu, H. Li, D. Du, X. Su and Y. Lin, *Anal. Chem.*, 2018, **90**, 2618-2624.
145. S. Qu, H. Chen, X. Zheng, J. Cao and X. Liu, *Nanoscale*, 2013, **5**, 5514-5518.
146. X. Cui, Y. Wang, J. Liu, Q. Yang, B. Zhang, Y. Gao, Y. Wang and G. Lu, *Sens. Actuators B Chem.*, 2017, **242**, 1272-1280.
147. W.-S. Zou, Q.-C. Zhao, J. Zhang, X.-M. Chen, X.-F. Wang, L. Zhao, S.-H. Chen and Y.-Q. Wang, *Anal. Chim. Acta*, 2017, **970**, 64-72.
148. A. Kumar, A. R. Chowdhuri, D. Laha, T. K. Mahto, P. Karmakar and S. K. Sahu, *Sens. Actuators B Chem.*, 2017, **242**, 679-686.
149. X. Li, Y. Zheng, Y. Tang, Q. Chen, J. Gao, Q. Luo and Q. Wang, *Spectrochim. Acta A*, 2019, **206**, 240-245.

View Article Online
DOI: 10.1039/C9NR05028K

150. M. Yang, W. Kong, H. Li, J. Liu, H. Huang, Y. Liu and Z. Kang, *Microchim. Acta*, 2015, **182**, 2443-2450.
151. A. Gupta, N. C. Verma, S. Khan and C. K. Nandi, *Biosens. Bioelectron.*, 2016, **81**, 465-472.
152. S. Sun, K. Jiang, S. Qian, Y. Wang and H. Lin, *Anal. Chem.*, 2017, **89**, 5542-5548.
153. C. Zhu, S. Yang, G. Wang, R. Mo, P. He, J. Sun, Z. Di, N. Yuan, J. Ding, G. Ding and X. Xie, *J. Mater. Chem. C*, 2015, **3**, 8810-8816.
154. H. Sun, L. Wu, W. Wei and X. Qu, *Mater. Today*, 2013, **16**, 433-442.
155. X. Miao, X. Yan, D. Qu, D. Li, F. F. Tao and Z. Sun, *ACS Appl. Mater. Interfaces*, 2017, **9**, 18549-18556.
156. W. Gao, H. Song, X. Wang, X. Liu, X. Pang, Y. Zhou, B. Gao and X. Peng, *ACS Appl. Mater. Interfaces*, 2018, **10**, 1147-1154.
157. C. Liu, D. Ning, C. Zhang, Z. Liu, R. Zhang, J. Zhao, T. Zhao, B. Liu and Z. Zhang, *ACS Appl. Mater. Interfaces*, 2017, **9**, 18897-18903.
158. L. Cao, X. Wang, M. J. Meziani, F. Lu, H. Wang, P. G. Luo, Y. Lin, B. A. Harruff, L. M. Veca, D. Murray, S. Y. Xie and Y. P. Sun, *J. Am. Chem. Soc.*, 2007, **129**, 11318-11319.
159. S. T. Yang, J. H. Liu, P. Wang, S. N. Yang, L. Ge, S. J. Yan and Y. P. P. Sun, *Chemistryselect*, 2018, **3**, 6374-6381.
160. S. Kim, Y. Choi, G. Park, C. Won, Y. J. Park, Y. Lee, B. S. Kim and D. H. Min, *Nano Res.*, 2017, **10**, 503-519.
161. S. Y. Lim, W. Shen and Z. Gao, *Chem. Soc. Rev.*, 2015, **44**, 362-381.
162. J. Zhang and S. H. Yu, *Mater. Today*, 2016, **19**, 382-393.
163. B. S. B. Kasibabu, S. L. D'souza, S. Jha, R. K. Singhal, H. Basu and S. K. Kailasa, *Anal. Methods*, 2015, **7**, 2373-2378.
164. Z. Y. Wang, H. Liao, H. Wu, B. B. Wang, H. D. Zhao and M. Q. Tan, *Anal. Methods*, 2015, **7**, 8911-8917.
165. W. Li, Y. Zheng, H. Zhang, Z. Liu, W. Su, S. Chen, Y. Liu, J. Zhuang and B. Lei, *ACS Appl. Mater. Interfaces*, 2016, **8**, 19939-19945.
166. P. Das, M. Bose, S. Ganguly, S. Mondal, A. K. Das, S. Banerjee and N. C. Das, *Nanotechnology*, 2017, **28**, 195501.
167. X. Zhai, P. Zhang, C. Liu, T. Bai, W. Li, L. Dai and W. Liu, *Chem. Commun.*, 2012, **48**, 7955-7957.
168. A. M. Chizhik, S. Stein, M. O. Dekaliuk, C. Battle, W. Li, A. Huss, M. Platen, I. A. Schaap, I. Gregor, A. P. Demchenko, C. F. Schmidt, J. Enderlein and A. I. Chizhik, *Nano Lett.*, 2016, **16**, 237-242.
169. X. T. Zheng, A. Ananthanarayanan, K. Q. Luo and P. Chen, *Small*, 2015, **11**, 1620-1636.
170. B. Kong, A. Zhu, C. Ding, X. Zhao, B. Li and Y. Tian, *Adv. Mater.*, 2012, **24**, 5844-5848.
171. Y. Cheng, C. Li, R. Mu, Y. Li, T. Xing, B. Chen and C. Huang, *Anal. Chem.*, 2018, **90**, 11358-11365.
172. Y. C. Song, W. Shi, W. Chen, X. H. Li and H. M. Ma, *J. Mater. Chem.*, 2012, **22**, 12568-12573.
173. C. H. Lee, R. Rajendran, M. S. Jeong, H. Y. Ko, J. Y. Joo, S. Cho, Y. W. Chang and S. Kim, *Chem. Commun.*, 2013, **49**, 6543-6545.
174. S. Ruan, J. Qian, S. Shen, J. Chen, J. Zhu, X. Jiang, Q. He, W. Yang and H. Gao, *Bioconjug. Chem.*, 2014, **25**, 2252-2259.
175. X. W. Zhao, J. L. Zhang, L. H. Shi, M. Xian, C. Dong and S. M. Shuang, *RSC Adv.*, 2017, **7**, 42159-42167.
176. N. Puvvada, B. N. Kumar, S. Konar, H. Kalita, M. Mandal and A. Pathak, *Sci. Technol. Adv. Mater.*, 2012, **13**, 045008.
177. W. J. Lu, X. J. Gong, Z. H. Yang, Y. X. Zhang, Q. Hu, S. M. Shuang, C. Dong and M. M. F. Choi, *RSC Adv.*, 2015, **5**, 16972-16979.

View Article Online
DOI: 10.1039/C9NR05028K

178. T. Pal, S. Mohiyuddin and G. Packirisamy, *ACS Omega*, 2018, **3**, 831-843.
179. Y. Cui and J. Irudayaraj, *Wiley Interdiscip. Rev. Nanomed. Nanobiotechnol.*, 2015, **7**, 387-407.
180. G. Lemenager, E. De Luca, Y. P. Sun and P. P. Pompa, *Nanoscale*, 2014, **6**, 8617-8623.
181. S. K. Das, Y. Liu, S. Yeom, D. Y. Kim and C. I. Richards, *Nano Lett.*, 2014, **14**, 620-625.
182. S. Khan, N. C. Verma, A. Gupta and C. K. Nandi, *Sci. Rep.*, 2015, **5**, 11423.
183. N. C. Verma, S. Khan and C. K. Nandi, *Methods Appl. Fluoresc.*, 2016, **4**, 044006.
184. H. Wang, Q. Ma, Y. Wang, C. Wang, D. Qin, D. Shan, J. Chen and X. Lu, *Anal. Chim. Acta*, 2017, **973**, 34-42.
185. S. T. Yang, L. Cao, P. G. Luo, F. Lu, X. Wang, H. Wang, M. J. Meziani, Y. Liu, G. Qi and Y. P. Sun, *J. Am. Chem. Soc.*, 2009, **131**, 11308-11309.
186. H. Tao, K. Yang, Z. Ma, J. Wan, Y. Zhang, Z. Kang and Z. Liu, *Small*, 2012, **8**, 281-290.
187. X. Huang, F. Zhang, L. Zhu, K. Y. Choi, N. Guo, J. Guo, K. Tackett, P. Anilkumar, G. Liu, Q. Quan, H. S. Choi, G. Niu, Y. P. Sun, S. Lee and X. Chen, *ACS Nano*, 2013, **7**, 5684-5693.
188. H. Y. Ko, Y. W. Chang, G. Paramasivam, M. S. Jeong, S. Cho and S. Kim, *Chem. Commun.*, 2013, **49**, 10290-10292.
189. T. Feng, X. Ai, G. An, P. Yang and Y. Zhao, *ACS Nano*, 2016, **10**, 4410-4420.
190. J. Tang, B. Kong, H. Wu, M. Xu, Y. Wang, Y. Wang, D. Zhao and G. Zheng, *Adv. Mater.*, 2013, **25**, 6569-6574.
191. P. Huang, J. Lin, X. Wang, Z. Wang, C. Zhang, M. He, K. Wang, F. Chen, Z. Li, G. Shen, D. Cui and X. Chen, *Adv. Mater.*, 2012, **24**, 5104-5110.
192. A. Kleinauskas, S. Rocha, S. Sahu, Y. P. Sun and P. Juzenas, *Nanotechnology*, 2013, **24**, 325103.
193. S. Khan, N. C. Verma, Chethana and C. K. Nandi, *ACS Appl. Nano Mater.*, 2018, **1**, 483-487.
194. T. Zhang, F. Zhao, L. Li, B. Qi, D. Zhu, J. Lü and C. Lü, *ACS Appl. Mater. Interfaces*, 2018, **10**, 19796-19805.
195. S. Paulo-Mirasol, E. Martínez-Ferrero and E. Palomares, *Nanoscale*, 2019, **11**, 11315-11321.
196. F. Yuan, Z. Wang, X. Li, Y. Li, Z. a. Tan, L. Fan and S. Yang, *Adv. Mater.*, 2017, **29**, 1604436.
197. X. Zhang, Y. Zhang, Y. Wang, S. Kalytchuk, S. V. Kershaw, Y. Wang, P. Wang, T. Zhang, Y. Zhao, H. Zhang, T. Cui, Y. Wang, J. Zhao, W. W. Yu and A. L. Rogach, *ACS Nano*, 2013, **7**, 11234-11241.
198. T. Feng, Q. Zeng, S. Lu, X. Yan, J. Liu, S. Tao, M. Yang and B. Yang, *ACS Photonics*, 2018, **5**, 502-510.
199. R. Genc, M. O. Alas, E. Harputlu, S. Repp, N. Kremer, M. Castellano, S. G. Colak, K. Ocakoglu and E. Erdem, *Sci. Rep.*, 2017, **7**, 11222.
200. X. Zhang, J. Wang, J. Liu, J. Wu, H. Chen and H. Bi, *Carbon*, 2017, **115**, 134-146.
201. G. Chen, S. Wu, L. Hui, Y. Zhao, J. Ye, Z. Tan, W. Zeng, Z. Tao, L. Yang and Y. Zhu, *Sci. Rep.*, 2016, **6**, 19028.
202. Y. Yang, X. Ji, M. Jing, H. Hou, Y. Zhu, L. Fang, X. Yang, Q. Chen and C. E. Banks, *J. Mater. Chem. A*, 2015, **3**, 5648-5655.
203. H. Hou, C. E. Banks, M. Jing, Y. Zhang and X. Ji, *Adv. Mater.*, 2015, **27**, 7861-7866.
204. X. Li, M. Rui, J. Song, Z. Shen and H. Zeng, *Adv. Funct. Mater.*, 2015, **25**, 4929-4947.
205. W. Kwon, S. Do, J.-H. Kim, M. Seok Jeong and S.-W. Rhee, *Sci. Rep.*, 2015, **5**, 12604.
206. J. Shao, S. Zhu, H. Liu, Y. Song, S. Tao and B. Yang, *Adv. Sci.*, 2017, **4**, 1700395.
207. Y. Wang, K. Wang, Z. Han, Z. Yin, C. Zhou, F. Du, S. Zhou, P. Chen and Z. Xie, *J. Mater. Chem. C*, 2017, **5**, 9629-9637.

View Article Online
DOI: 10.1039/C9NR05028K

208. X. Miao, D. Qu, D. Yang, B. Nie, Y. Zhao, H. Fan and Z. Sun, *Adv. Mater.*, 2018, **30**, 1704740.
209. F. Wang, M. Kreiter, B. He, S. Pang and C.-y. Liu, *Chem. Comm.*, 2010, **46**, 3309-3311.
210. X. Guo, C.-F. Wang, Z.-Y. Yu, L. Chen and S. Chen, *Chem. Comm.*, 2012, **48**, 2692-2694.
211. L.-H. Mao, W.-Q. Tang, Z.-Y. Deng, S.-S. Liu, C.-F. Wang and S. Chen, *Ind. Eng. Chem. Res.*, 2014, **53**, 6417-6425.
212. X. Li, S. P. Lau, L. Tang, R. Ji and P. Yang, *J. Mater. Chem. C*, 2013, **1**, 7308-7313.
213. M. Shamsipur, A. Barati and S. Karami, *Carbon*, 2017, **124**, 429-472.
214. F. Wang, Y.-h. Chen, C.-y. Liu and D.-g. Ma, *Chem. Comm.*, 2011, **47**, 3502-3504.
215. J. Zhang and S.-H. Yu, *Mater. Today*, 2016, **19**, 382-393.

Table of Contents: